British Columbia Geological Survey
Geological Fieldwork 2000

# Preliminary Fluid Inclusion Study of Quartz Vein and Massive-Banded-Stringer Pyrite Mineralization in the Wells-Barkerville Gold Belt, East-Central British Columbia

By Kathryn P.E. Dunne[1] and Gerry E. Ray[2]

***KEYWORDS:*** Economic geology, quartz veins, massive-banded-stringer pyrite ore, gold, fluid inclusions, salinity, homogenization temperature, Wells, Barkerville, Island Mountain mine, Mosquito Creek mine, Cariboo Gold Quartz mine, Bonanza Ledge zone.

## INTRODUCTION

The Wells-Barkerville Gold Belt lies approximately 65 km east of Quesnel, in the Cariboo Mining Division, British Columbia. Gold in this area is hosted by two types of mineralization: quartz-pyrite vein and massive-banded-stringer pyrite ore. Both types are hosted by a lower greenschist facies stratigraphic interval within clastic metasedimentary rocks of the Barkerville subterrane.

This paper is the first publication of fluid inclusion data from the belt. The objectives of this study are to:

- document fluid inclusion characteristics (i.e. temperature, composition) in quartz from both vein and 'massive' pyritic mineralization at the Mosquito Creek and Island Mountain mines, and from quartz vein mineralization at the Cariboo Gold Quartz mine, and the BC, Warspite and Perkins vein occurrences (Figure 1).
- compare fluid inclusion characteristics of vein and massive-banded-stringer ore within and between deposits in the belt.
- compare fluid inclusion data from the Wells-Barkerville Belt with data from other gold districts hosted in low metamorphic-grade rocks.
- discuss the use of fluid inclusion data as a tool to determine the depositional environment of deposits in the Wells-Barkerville Belt.

## GEOLOGICAL SETTING

The Wells-Barkerville Belt is within the Barkerville subterrane of the Late Proterozoic and Paleozoic Kootenay Terrane. The Barkerville subterrane comprises metamorphosed grit, quartzite, phyllite, lesser limestone and volcaniclastic rocks of the Snowshoe Group (Struik, 1988). Quartz-pyrite vein and massive, banded and stringer pyritic mineralization in the Wells-Barkerville Belt are confined to a lower greenschist facies stratigraphic interval within the upper Snowshoe Group variably termed the 'Baker and Rainbow Members" (Hansen, 1935), Snowshoe Formation (Sutherland-Brown, 1957) and Downey and Hardscrabble successions (Struik, 1988).

Isoclinal to tight folds and shear zones record conditions of early ductile flow in the Barkerville Subterrane (Struik *et al.,* in Gabrielse, 1991). Open folds and faults characteristic of brittle conditions are superimposed on the ductile structures (Struik op. cit.). A progressive sequence of veining at the Cariboo Gold Quartz, Island Mountain and Mosquito mines spans early veins formed during the dominant phase of ductile deformation and later least strained veins that contain most of the gold (Rhys and Ross, 2000; Rhys, 2000).

## MINERAL DEPOSITS

Two types of gold-bearing ore occur in the Wells-Barkerville Belt: quartz-pyrite veins and massive-banded-stringer pyrite (Johnson and Uglow, 1926; Hanson, 1935; Benedict, 1945; Skerl, 1948; Richards, 1948; Sutherland-Brown, 1957; Alldrick, 1983; Robert and Taylor, 1989). McTaggart and Knight (1993) suggest that gold from the 'massive' pyritic ore at Island Mountain and Mosquito Creek mines (average fineness of 870) differs from gold in quartz veins at the Cariboo Gold Quartz mine (fineness of 945). Production figures from the Island Mountain mine indicate that gold grades in the 'massive' ore are higher than grades in the 'vein' ore (Benedict, 1945).

Vein ore typically comprises dominantly massive, white to translucent quartz, lesser dolomite/ankerite, muscovite (as sericite) and pyrite and rarely minor arsenopyrite, galena, sphalerite and/or scheelite (cf. Skerl, 1948). Pyrrhotite and chalcopyrite have been reported as accessory minerals (Skerl, op. cit.; International Wayside Gold Mines Ltd., 2000). Wide veins, such as the BC Vein, can be greater than 15 metres in width and may have sheared graphitic margins. Sericite from quartz veins in the Cariboo Gold Quartz mine, Mosquito Creek Gold mine and Cariboo Hudson mine have been dated using the

---

[1] *Consulting Geologist*

[2] *British Columbia Ministry of Energy and Mines*

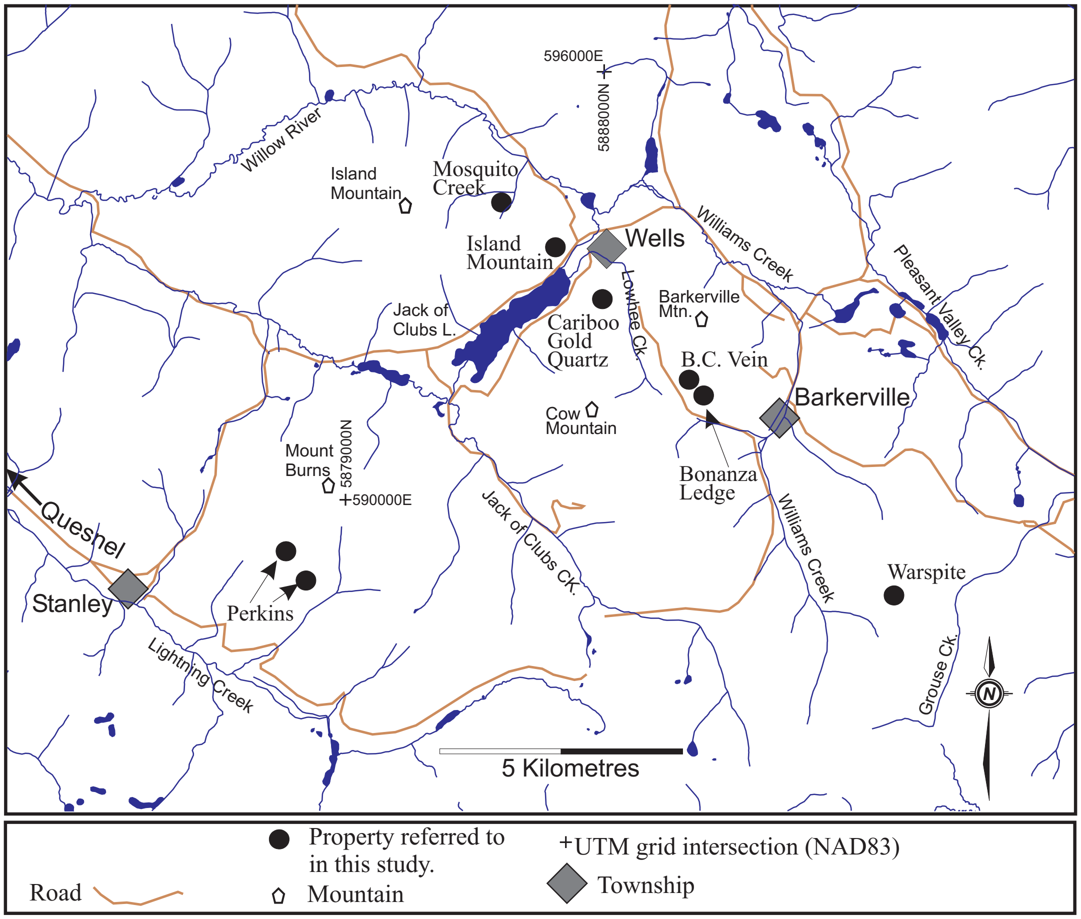

Figure 1. Location map of properties sampled and referred to in this study, Wells-Barkerville area.

K-Ar method at 140 Ma (International Wayside Gold Mines Ltd., 2000).

Vein textures in the Wells-Barkerville Belt are highly variable. Massive, white to translucent 'bull' quartz veins comprise subhedral to anhedral crystals from less than 0.5 mm to approximately 2 mm in size. Sutured grain boundaries have been noted in some samples. Many of the massive veins are highly fractured (Photo 1) and in some cases the abundance of microfractures results in a texture described by Reynolds (1991) as 'wispy quartz' (Photo 2). Reynolds (op. cit.) suggests that this texture is characteristic of deep vein environments (> 4km and possibly > 8 km). In contrast, breccia textures indicative of brittle crushing reflecting higher level emplacement are observed in other veins (Photos 3 and 4). Skerl (1948) reports that approximately 1 percent of the veins at the Cariboo Gold Quartz deposit have vugs containing well terminated quartz crystals. These vugs indicate open-space filling late in the vein history. They have been noted in veins elsewhere in the Wells-Barkerville Belt (*eg*. Mosquito Creek, Warspite, Perkins). The quartz crystal terminations are typically translucent whereas most of the massive quartz is white due to abundant fluid inclusions along microfractures. Even fractured and wispy quartz veins have vugs (*cf*. Photo 2 - centre). Differences in temperature and composition between the late (?), open-space fill quartz and the earlier massive quartz are described below.

Four distinct, structurally-controlled vein orientations occur in the Wells-Barkerville Belt: strike, bedding-parallel veins (NW-SE/45-70NE), northerly (N-S/40-70E), orthogonal (030-040/70SE) and diagonal (070-090/subvertical) (Hanson, 1935; Benedict, 1945; Richards, 1948; Skerl, 1948; Robert and Taylor, 1989). Orthogonal veins are most abundant and these contain the highest concentrations of gold (Benedict, 1945, Robert and Taylor, 1989, International Wayside Gold Mines Ltd., 2000).

Two distinct styles of pyritic ore mineralization are evident in the belt. At Mosquito Creek and Island Mountain mines the pyritic orebodies occur within or adjacent to limestone units (Benedict, 1945; Alldrick, 1983), but at Bonanza Ledge in carbonaceous metasedimentary units and limestone (Rhys and Ross, 2000; Rhys, 2000). Pyrite orebodies at Mosquito Creek and Island Mountain mines tend to be commonly associated with fold hinges. Stope dimensions for these orebodies in fold hinges are commonly less than 10 metres thick and several hundred metres in the down plunge direction (Benedict, 1945, Robert and Taylor, op. cit.). Pyrite lenses at Mosquito

Photo 1. Highly fractured 'bull' quartz vein, Cariboo Gold Quartz deposit. Note open vug lined with quartz crystals top right of photo. Sample CGQ-FI-3. Transmitted plane light. Width of photo 2mm.

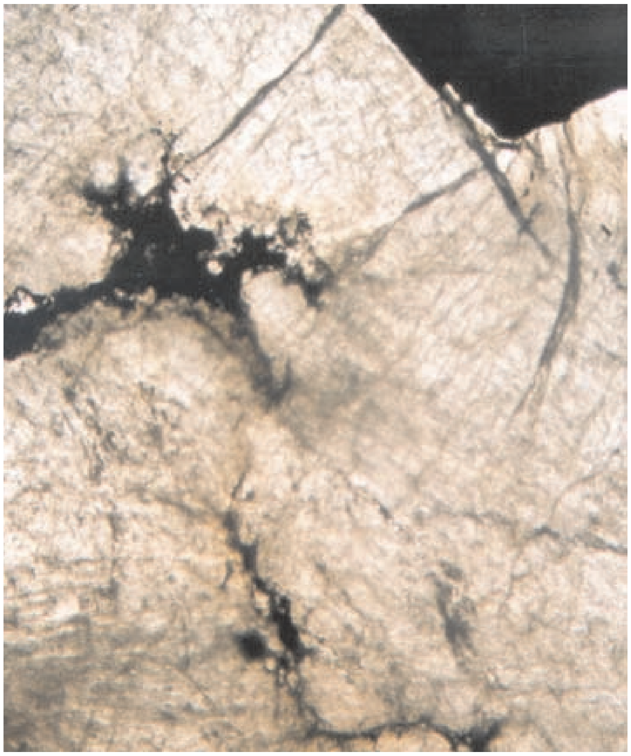

Photo 2. Abundant 'sweeping' microfractures giving appearance of wispy quartz texture in quartz-pyrite-sphalerite vein, Warspite occurrence. Note large vug left of centre. Sample GR-00-81. Transmitted plane light. Width of photo 2mm.

Photo 3. Quartz breccia with angular fragments from 0.5 to 2 cm provides evidence of brittle deformation near footwall of BC Vein above Bonanza Ledge. Open-space filling with clear euhedral quartz crystals is noted in this sample. Sample GR-00-46. Transmitted plane light. Width of photo 18.5 mm.

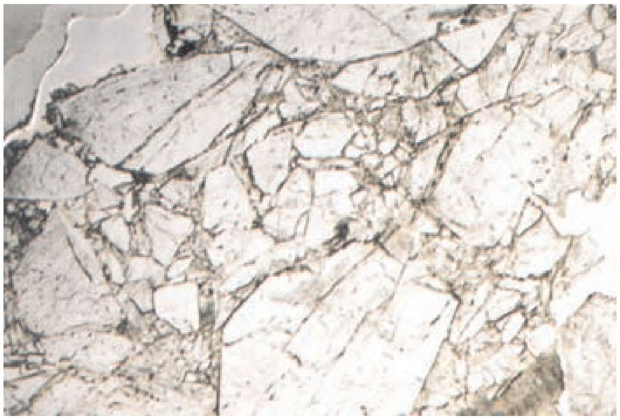

Photo 4. Quartz breccia with angular fragments of clear euhedral quartz from open vugs, Mosquito Creek deposit. Sample GR-00-73. Transmitted plane light. Width of photo 18.5 mm.

Creek can either be parallel to the strong foliation or parallel to the bedding (Robert and Taylor, 1989). At the Bonanza Ledge zone, Rhys (2000) describes folded high-grade pyrite mineralization that is discordant to stratigraphy and locally more than 30 metres thick over a strike length of 130 metres.

Pyritic ore at Bonanza Ledge comprises veinlets, concordant laminations and massive bands of pyrite, often with trace chalcopyrite and galena, in a gangue of muscovite, dolomite/ankerite and quartz (Rhys and Ross, 2000; Rhys, 2000). Pyrite orebodies at Mosquito Creek typically comprise fine to medium-grained crystalline pyrite forming individual or stacked lenses (Robert and Taylor, 1989). At the Cariboo Gold Quartz mine, massive crystalline pyrite orebodies contain little or no quartz but grey and white carbonates, galena, sphalerite and scheelite are reported around the margins of the ore (Skerl, 1948). Examples of the massive and banded pyrite ore from the Island Mountain mine in a gangue of fine-grained quartz, sericite and minor carbonate are in Photos 5 and 6.

Quartz in the massive pyritic Bonanza Ledge ore occurs as subhedral to anhedral crystals from about 0.25 mm to 1.5 mm in size, or as finer-grained, possibly recrystallized crystals that are mostly < 0.15 mm in diameter, with sutured grain boundaries (C. Leitch, written communication to G.E. Ray, October 2000). Undulose extinction indicative of strain is common in the larger crystals (C. Leitch, op. cit.). Similar quartz textures are evident in a limited number of samples collected from Mosquito Creek and Island Mountain deposits.

Most workers in the Wells-Barkerville Belt (Hanson, 1935; Benedict, 1945; Skerl, 1948; Sutherland-Brown, 1957; Alldrick, 1983; Rhys and Ross, 2000; Rhys, 2000) believe that the pyrite lenses formed by replacement of carbonate units. A syn-sedimentary origin has also been proposed by Robert and Taylor (1989).

## FLUID INCLUSION DATA

This preliminary paper describes fluid inclusions in quartz in the quartz-pyrite veins and in the massive-banded-stringer pyrite. Samples were examined from the Warspite, Cariboo Gold Quartz, Island Mountain, Mosquito Creek, and Perkins properties (Figure 1). The former Cariboo Gold Quartz, Island Mountain and Mosquito Creek mines were the principal lode gold producers in the belt. Description of the geology of the deposits have been given by Hanson (1935), Benedict (1945), Holland (1948), Johnson and Uglow (1926), Skerl (1948), Richards (1948) and Sutherland-Brown (1957). Where possible, samples were taken from surface outcrops, underground exposures and drillcore. However, as some mine workings are inaccessible, a number of samples were collected from dumps adjacent to portals. Over 30 'quick plates' were prepared for fluid inclusion petrography. Quick plates are thick sections, 80 to 100 microns thick, mounted on glass slides with epoxy and polished on the top surface only. Of these, 12 samples, 2 from each of the 5 properties listed above and 2 from the BC Vein were selected for fluid inclusion microthermometry and re-prepared as doubly-polished sections. Samples were selected to give broad representation of both types of mineralization and, for veins, to give representation of some of the four vein orientations (Table 1).

Quartz was used for microthermometry because it has high tensile strength and is relatively translucent. Sphalerite is another high tensile strength mineral and is preferable to quartz because it is a sulphide mineral. Sphalerite is present in the BC Vein in the hanging-wall of the Bonanza Ledge zone (Ray *et al.*, 2001, this volume) but unfortunately the mineral in the sample (GR-00-91) is too opaque for fluid inclusion study. Future work in the belt should focus on the potential of sphalerite and scheelite for fluid inclusion microthermometry.

Fluid inclusions were evaluated using the concept of fluid inclusion assemblages (FIA's). This ensures that the data was not biased by samples containing large numbers of fluid inclusions and helps to eliminate inconsistent data caused by changes in mass, volume or shape of inclusions after entrapment (i.e. eliminate non-representative inclusions that are the result of diffusion, stretching, or necking-down processes). A fluid inclusion assemblage (FIA) is a petrographically-associated group of inclusions such as those aligned along primary growth zones or secondary fracture planes. One representative data point, rather than several data points is used for each FIA.

### Petrography

Fluid inclusions in quartz from both vein and 'massive' ore in our Wells-Barkerville samples are typically less than 15 microns in longest dimension with inclusions in 'massive' ore usually less than 6 microns in longest dimension. Inclusions in some vein samples reach 30 microns in longest dimension. They vary in shape from irregular to smooth and in some cases they mimic the host crystal form and are 'negative-crystal'-shaped.

Fluid inclusions in our vein samples are classified as secondary or indeterminate. Secondary inclusions are aligned along fractures that crosscut grain boundaries

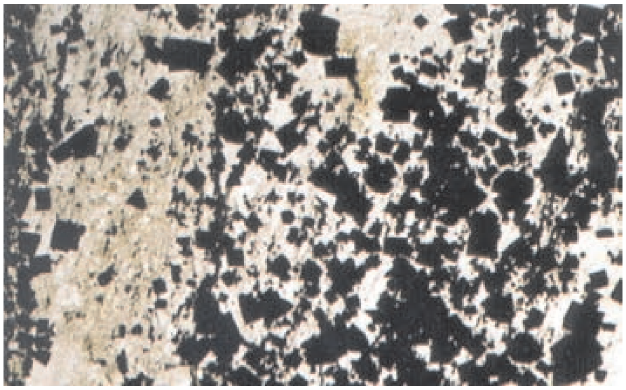

Photo 5. Medium-grained crystalline pyrite (black), quartz and minor fine-grained sericite representative of 'massive' ore, Island Mountain deposit. Sample GR-00-85. Transmitted plane light. Width of photo 18.5 mm.

Photo 6. Fine and medium-grained crystalline pyrite (black), quartz, minor sericite and carbonate representative of 'banded' ore, Island Mountain deposit. Sample GR-00-88. Transmitted plane light. Width of photo 18.5 mm.

## TABLE 1
## SUMMARY DESCRIPTIONS OF SAMPLES USED FOR FLUID INCLUSION MICROTHERMOMETRIC ANALYSES, WELLS-BARKERVILLE GOLD BELT

| DEPOSIT NAME | SAMPLE NUMBER | ORE TYPE | STRUCTURE TYPE | LOCATION IN VEIN | VEIN TEXTURES | MINERALS[1] |
|---|---|---|---|---|---|---|
| Cariboo Gold Quartz (mine) | CGQ-FI-3 | vein | orthogonal? | ? | bull qz | qz |
|  | CGQ-FI-4 | vein | ? | whole vein | bull qz | qz |
| BC Vein (Bonanza Ledge) | GR-00-91 | vein | strike | footwall | massive | sph<br>qz |
| BC Vein | GR-00-46 | vein | strike | margin | bx, vugs | qz |
| Island Mountain (mine) | GR-00-85 | massive |  |  | massive/banded | py,qz,ser |
|  | GR-00-94 | vein | diagonal | ? | recry. qz<br>bull qz | gal,qz |
| Mosquito Creek (mine) | GR-00-67 | vein | strike | centre of 1 m thick vein | vugs | qz |
|  | GR-00-68 | massive |  |  | banded/stringer<br>recry. qz | py, qz |
| Warspite (veins) | GR-00-81 | vein | dump | ? | bull qz | py, sph, qz |
|  | GR-00-82 | vein | dump | ? | bull qz | gal, qz |
| Perkins (veins) | GR-00-49 | vein | dump | ? | vugs | qz |
|  | GR-00-56 | vein | orthogonal? | ? | vugs | qz |

1. Mineral abbreviations: qz=quartz, py=pyrite, sph=sphalerite, gal=galena, ser=sericite

(Roedder, 1984). Interpretation of secondary fluid inclusion data reflects the conditions of formation of post-crystal formation fluids trapped in fractures after crystal growth ceased. No gold particles were seen with any fluid inclusions in this study but gold is reported to be directly associated with secondary fluid inclusions in quartz veins at the Sigma Mine in Quebec (Robert and Kelly, 1987). Further detailed petrographic work is required to evaluate the occurrence of gold with respect to fluid inclusion chronology in the quartz veins of the Wells-Barkerville Belt.

The fluid inclusions noted in our 'massive' pyrite ore samples are classified as primary, secondary, pseudosecondary or indeterminate, based on the criteria of Roedder (1984) and Bodnar *et al.* (1985). Primary fluid inclusions are aligned along growth zones in quartz proximal to sulphide grains in 'massive' ore from the Mosquito Creek deposit (Photos 7 and 8). Unfortunately, these primary inclusions are less than 1-2 microns long and are too small for heating-freezing work. However, slightly larger primary and pseudosecondary fluid inclusions trapped in quartz in recrystallized zones around pyrite in 'massive' ore from the Island Mountain and Mosquito Creek deposits have been observed and measured (Photos 5, 9, 10 and 11). Pseudosecondary fluid inclusions (Photos 11 & 12) are aligned along fractures that do not crosscut grain boundaries and are presumed to represent fluids trapped in fractures at the time the crystal was growing (Roedder, 1984).

The occurrence of primary and pseudosecondary fluid inclusions in our samples is unusual because typically, in deposits hosted by metamorphosed and deformed rocks, significant deformation of quartz leads to recrystallization and expulsion of inclusions as well as cracking and trapping of secondaries, which may be subsequently annealed out (*cf.* Yardley, 1999). However, some studies report that the quartz grains are not completely recrystallized. For example, Garba and Akande (1992) document primary fluid inclusions in vein quartz hosted by metasediments in the Zuru Schist Belt of northwestern Nigeria. Primary fluid inclusions have also been documented in euhedral quartz encapsulated in sulphide grains at the Sigma mine in Quebec (Guha *et al.*, 1991).

The primary and pseudosecondary fluid inclusions documented in this study have relatively consistent liquid-to-vapour ratios but moderately variable homogenization temperatures. The variability in homogenization temperature data may be due to thermal re-equilibration as suggested by Smith and Yardley (1999), undetectable necking down (post-entrapment change in inclusion shape) or real variability in the FIA's. Further petrographic work on additional 'massive' ore samples at a number of deposits in the Wells-Barkerville Belt is required to assess whether the primary inclusions represent fluids formed syn-crystallization or whether the primary inclusions show the effects of leakage or decrepitation.

In the Wells-Barkerville Belt, four compositional types of fluid inclusions have been identified in quartz from both vein and 'massive' ore in the Wells-Barkerville Belt through observation of phases present and volume percent of phases at room temperature. For each measured fluid inclusion type within a fluid inclusion assem-

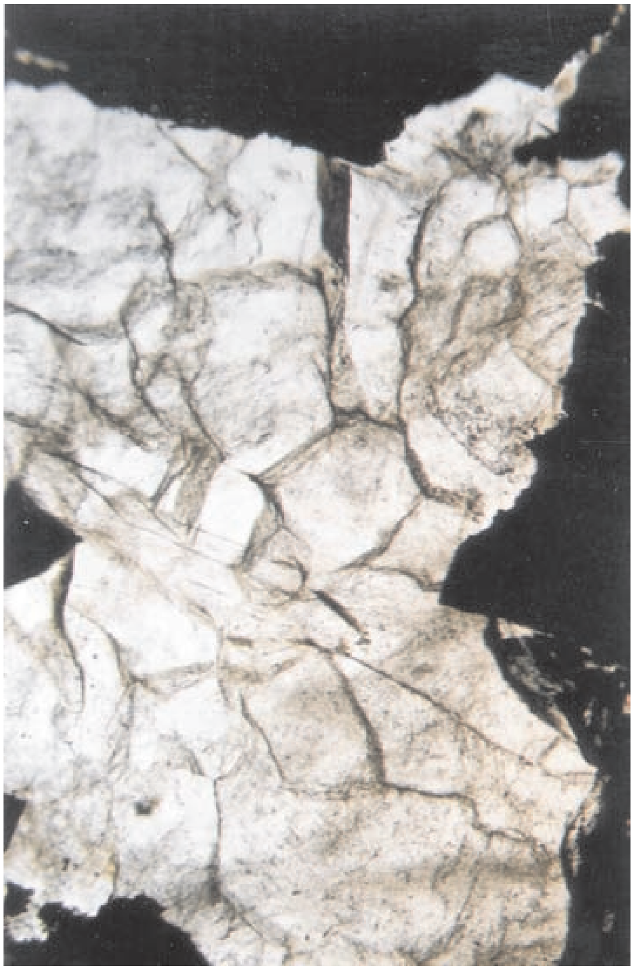

Photo 7. Subhedral to anhedral quartz crystals adjacent to medium-grained crystalline pyrite (black) in 'massive' ore, Mosquito Creek deposit. Evidence of quartz recrystallization? seen as fine-grained quartz crystals with 120°C grain boundaries at top right of photo. Note area of enlargement for Photo 8 is top right of photo 7. Sample GR-00-68. Transmitted plane light. Width of photo 2mm.

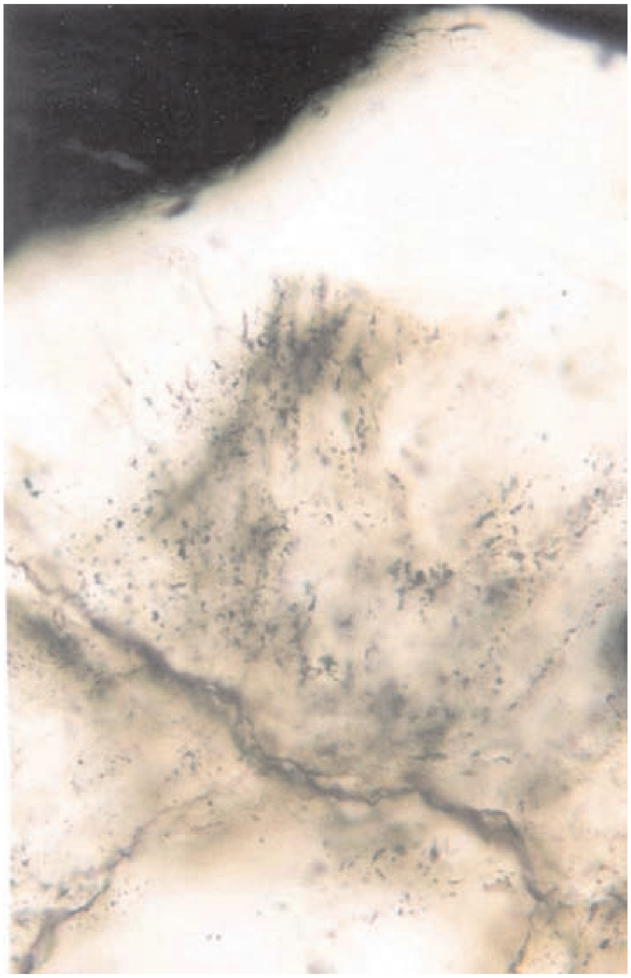

Photo 8. Tiny (<1 micrometre) primary fluid inclusions aligned along growth zones in quartz proximal to medium-grained pyrite in 'massive' ore, Mosquito Creek deposit. This photo is an enlargement of top right of Photo 7. Sample GR-00-68. Transmitted plane light. Width of photo 400 µm.

blage (FIA), the liquid-to-vapour ratios were relatively consistent (±20 volume percent vapour). The compositional types, based on phases present at room temperature (20°C), modified from the nomenclature of Nash (1976) are: two-phase aqueous liquid-rich (Type I), multiphase (Type III), two and three-phase mixed aqueous and $CO_2$-rich (Type IV) and monophase vapour $CO_2$-$CH_4$ (Type V).

Type I fluid inclusions are characterised by 2 aqueous phases, liquid and vapour (Photo 12). The vapour phase typically comprises approximately 5 volume percent of the inclusion but rarely 10, 20 and 30 volume percent vapour have been observed. Type I fluid inclusions have been noted in all samples except in quartz from the Perkins occurrence.

Type III inclusions comprise a liquid brine, vapour and one or more solid phases (Photo 13). The vapour phase typically comprises approximately 10 to 30 volume percent of the inclusion. Many of the solid phases are dominantly translucent and cubic and therefore are presumed to be salts. Confirmation of the identity of the solid phases as salts has not been possible as fluid inclusions containing these phases decrepitate prior to solid phase dissolution. In some cases, secondary planes of type III inclusions with comparable phases present have been observed, although some 'isolated' type III inclusions may have formed by accidental trapping of the solid phases or post-entrapment changes in the inclusions. Type III inclusions have been noted in quartz veins from the Cariboo Gold Quartz, BC Vein and Perkins mineral occurrences and in quartz associated with 'massive' ore at the Mosquito Creek deposit. Limited freezing and subsequent melting behaviour of type III fluid inclusions in quartz from the Perkins occurrence indicates a $CO_2$-bearing vapour phase (*see* below).

Type IV inclusions consist of 2 or 3 phases at room temperature. These are either an aqueous liquid and $CO_2$-bearing liquid (Photo 14) or an outer aqueous liquid, inner $CO_2$-bearing liquid and a $CO_2$-bearing vapour (Photo 15). The $CO_2$ volumetric proportions of Type IV

Photo 9. Recrystallized quartz zone, approximately 0.5 mm wide, with virtually no fluid inclusions, around medium-grained pyrite (black) in massive ore, Mosquito Creek deposit. Note area of enlargement for Photo 11 is right of centre of Photo 9. Sample GR-00-68. Transmitted plane light. Width of photo 2mm.

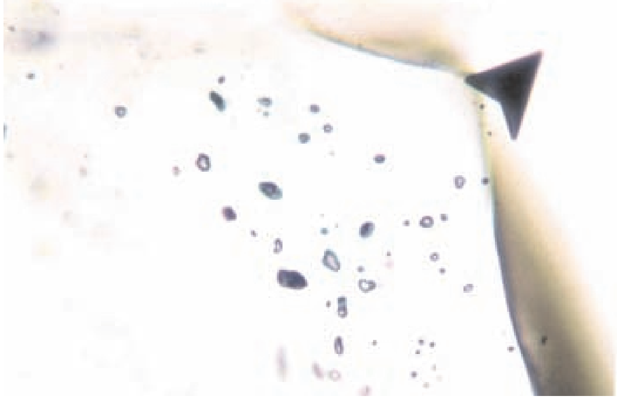

Photo 11. Pseudosecondary fluid inclusions aligned along fractures in recrystallized quartz proximal to pyrite crystals (black), 'massive' ore, Mosquito Creek deposit. Note occurrence of 2 phase liquid-rich and monophase vapour-rich fluid inclusions trapped in the same healed fracture. This photo is an enlargement of area right of centre of Photo 9. Sample GR-00-68. Transmitted plane light. Width of photo 300 µm.

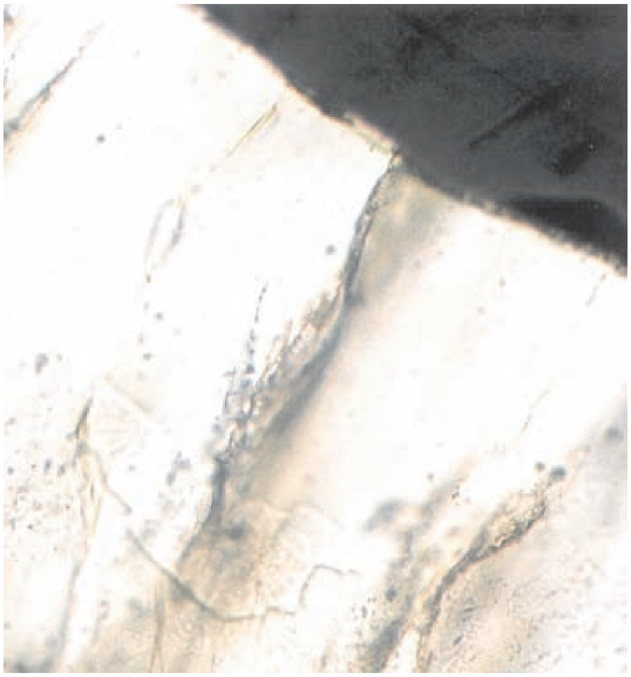

Photo 10. Recrystallized quartz zone, approximately 0.3 mm wide, around medium-grained crystalline pyrite (black) in 'massive' ore, Island Mountain deposit. Recrystallized zone comprises less than one percent tiny fluid inclusions. Sample GR-00-85. Transmitted plane light. Width of photo 340 µm.

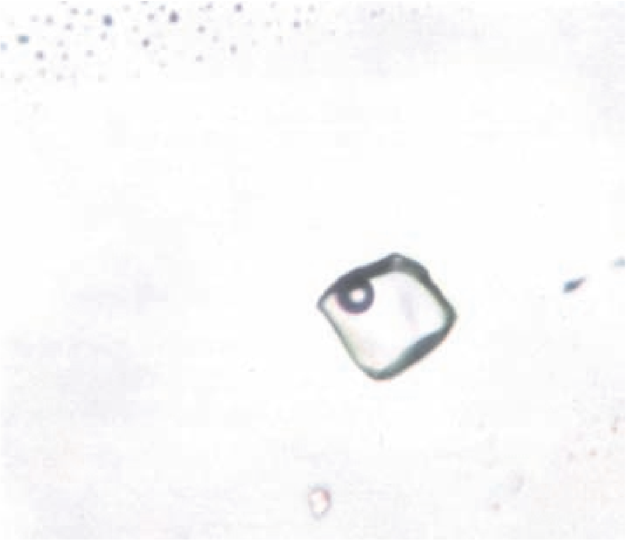

Photo 12. Negative crystal - shaped Type I fluid inclusions characterized by 2 aqueous phases: liquid and vapour in vein quartz, Mosquito Creek deposit. Sample GR-00-67. Transmitted plane light. Width of photo 160 µm.

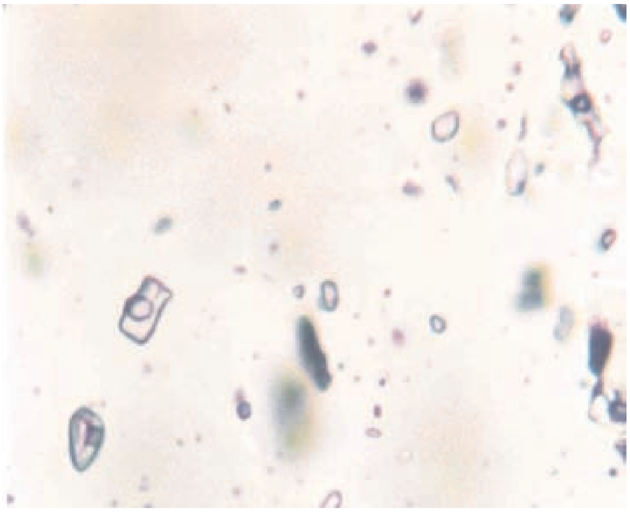

Photo 13. Smooth to negative crystal - shaped Type III fluid inclusions in a massive ‘bull’ quartz vein, Cariboo Gold Quartz deposit. Note solid ‘daughter’ crystals in the fluid inclusions left of centre and far right. Sample CGQ-FI-4. Transmitted plane light. Width of photo 160 µm.

inclusions range from 5 percent to 90 percent with 20 to 30 percent most typical. Type IV inclusions have been noted in all samples except GR-00-91(BC Vein) and GR-00-94 (Island Mountain vein).

Type V inclusions are typically very dark and consist of a single vapour phase at room temperature (Photo 14). Freezing and subsequent melting behaviour of these inclusions indicate the presence of $CO_2$-$CH_4$±$N_2$ phases. Type V fluid inclusions in quartz have been noted in all samples except in ‘massive’ pyritic ore from the Island Mountain mine and in veins from the Perkins occurrence.

Two phase liquid-rich Type IV inclusions are coeval with monophase vapour-rich Type V inclusions in secondary and pseudosecondary fracture planes in quartz from both vein and massive ore (Photos 11and 14). The coexistance of $CO_2$-bearing liquid-rich inclusions with variable liquid-to-vapour ratios and vapour-rich inclusions in the same fracture plane indicates that local effervescence occurred.

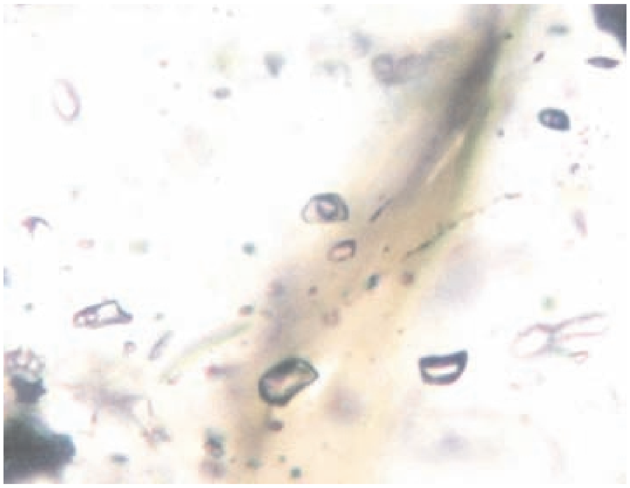

Photo 14. Coexisting monophase vapour-rich Type V inclusions and two phase liquid-rich Type IV inclusions aligned along a secondary fracture plane in quartz from a massive ‘bull’ quartz vein, Cariboo Gold Quartz deposit. Sample CGQ-FI-3. Transmitted plane light. Width of photo 160 µm.

## Microthermometric Data

Microthermometric data were obtained using a Fluid Inc. adapted USGS gas-flow heating-freezing stage housed at the Mineral Deposit Research Unit, Department of Earth and Ocean Sciences, University of British Columbia. Calibration of the stage was achieved using commercial Syn Flinc synthetic fluid inclusions and ice with the following accuracies: at -56.6±0.2°C, 374.1±0.6°C and 0.0±0.1°C. Temperatures of phase changes are presented for each fluid inclusion type from lowest to highest. Variation in final aqueous homogenization temperature with respect to fluid inclusion origin, deposit type and comparison between deposits are illustrated.

### *TYPE I FLUID INCLUSIONS*

Temperatures of first melting were obtained on 15 fluid inclusions from 4 samples representing both vein and ‘massive’ styles of mineralization (Figure 2). First melting temperatures range from -28.6°C to -20.0°C, with an average of -23.1°C. No systematic differences were

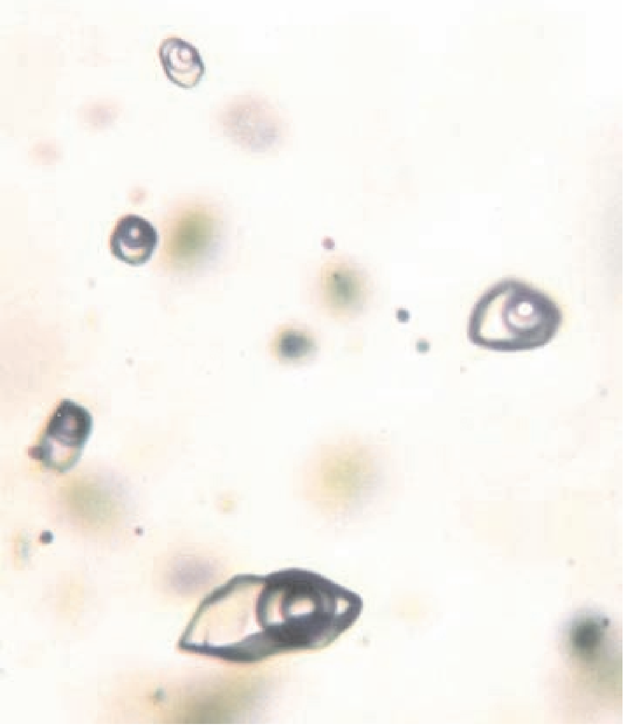

Photo 15. Smooth to negative - crystal shaped Type IV fluid inclusions in quartz from a quartz vein, Mosquito Creek deposit. Note the three $CO_2$ and $H_2O$ phases present at room temperature (20°C). Sample GR-00-67. Transmitted plane light. Width of photo 160 µm.

noted between vein and 'massive' styles of mineralization.

First melting temperature approximates the eutectic temperature of the salt-water mixtures. The observation of first melting below -21.2°C, the stable NaCl-$H_2O$ eutectic, indicates the addition of small concentrations of K+, $Ca_2$+, $Mg_2$+ or other ions to an $H_2O$-NaCl fluid. For the purposes of this preliminary study, the type I fluid is modelled as an NaCl brine partly because most formational fluids are NaCl-dominant (Goldstein and Reynolds, 1994) and because comparison of the cotectic surfaces where ice melts for various systems (Figure 6, from Crawford, 1981) shows only relatively small variations (< 5 wt.% change).

Temperatures of final ice melting were obtained from 30 fluid inclusions from the same and additional samples as the first melting temperatures (Figure 2). Final melting temperatures range from -9.2°C to -0.2°C, with an average of -3.3°C. Salinities calculated from final melting temperatures and the equation of Bodnar (1993) range from 0.4 to 13.1 weight percent NaCl equivalent (wt. percent NaCl equiv.) and average 5.4 wt. percent NaCl equiv. No systematic differences were noted between vein and 'massive' styles of mineralization. Metastable hydrate melting (possible hydrohalite) is observed from 0 to 10°C after ice melting.

Final homogenization temperatures of the inclusions, always to the liquid phase, were obtained on 39 Type I fluid inclusions from the same samples and some additional samples as the freezing data (above). Homogenization temperatures range from 101.1 to 298.8°C and average 168.9°C (Figure 3). Five fluid inclusions in quartz vein samples from the Cariboo Gold Quartz mine and BC Vein exhibited decrepitation of fluid inclusions prior to homogenization at temperatures between 150 and 300°C

## TYPE III FLUID INCLUSIONS

Limited data (4 data points) on freezing and subsequent melting behaviours of Type III fluid inclusions in quartz from the Perkins vein parallel the behaviour of $CO_2$-bearing Type IV fluid inclusions (see below). On heating, the solid phases do not melt prior to decrepitation (leakage) of the fluid inclusions at temperatures ranging from 220 to 258°C. Homogenization of one type III inclusion was achieved at 224°C, within the range for Type IV fluid inclusions (*see* below), prior to inclusion decrepitation at 250°C.

It is not known whether the Type III inclusions contain minerals that are true 'daughter' minerals or if the minerals are trapped accidental solids or are the result of 'necking down'. If the solids are salts and true 'daughter' minerals, this combination of salt-saturated and $CO_2$-bearing fluids trapped within inclusions in quartz veins at the Perkins veins has rarely been documented in fluid inclusion literature.

## TYPE IV FLUID INCLUSIONS

On freezing of the inclusions, phase separation of the vapour bubble into $CO_2$-liquid and $CO_2$-vapour phases occurred at about +5 to + 25°C. Further cooling resulted in freezing of the $H_2O$ phase at about -35 to -50°C and the $CO_2$ phase at about -90 to -95°C. Temperatures of $CO_2$ melting were obtained on 50 fluid inclusions from both vein and 'massive' styles of mineralization. Carbon dioxide melting temperatures typically range from -61.4 to -56.6°C with an average of -57.5°C (Figure 4). The average $CO_2$ melt temperature of -57.5°C indicates that < 4 mole percent or virtually no $CH_4$ or $N_2$ is dissolved in the $CO_2$. Type IV fluid inclusions can therefore be modelled using an $H_2O$-$CO_2$-NaCl system. Carbon dioxide-melting temperatures in quartz from the Perkins veins are much lower (Figure 3). These inclusions comprise from 0 to 20 mole percent $CH_4$ dissolved in the $CO_2$ using VX diagrams of Thiery *et al.* (1994).

Temperatures of clathrate (gas hydrate) melting were obtained on 47 fluid inclusions from the same samples as the $CO_2$-melting temperatures. Clathrate melting, which occurs after ice melting, varies from 0.2 to 9.8°C with an average of 6.6°C (Figure 4). Clathrate melting temperatures less than +10°C are another indication of very low $CH_4$ or $N_2$ presence in Type IV inclusions. Clathrate melting temperatures in excess of + 10°C are related to $CH_4$ impurities (Burruss, 1981). Salinities calculated from clathrate melting using the MacFlincor computer program (Brown and Hagemann, 1994) range from 1.4 to 15.7 wt. percent NaCl equiv.

Homogenization temperatures of $CO_2$ liquid and vapour were obtained from 45 fluid inclusions from the same samples as $CO_2$-melting and clathrate melting temperatures. Homogenization of the inclusions (always to the liquid phase) ranges from 5.6 to 30.5°C with an average of 19.7°C (Figure 4) which combined with volume estimates indicate a range in density of 0.54 to 0.84 grams per cubic centimetre for the $CO_2$ component of the inclusions.

Final homogenization temperatures of the inclusions, again always to the aqueous phase, were obtained on 36 Type IV fluid inclusions from the same samples as the freezing data (above). Homogenization temperatures range from 124.7 to 341.9°C and average 241.1°C (Figure 3). A large proportion, approximately one-third, of all Type IV inclusions decrepitate at temperatures ranging from 150 to 300°C prior to homogenization. This large proportion occurred irrespective of reasonable heating rates which were reduced to 5 degrees per minute in an attempt to lower the number of failed homogenization temperatures. Figure 3 shows that overall, Type IV fluid inclusions homogenize at significantly higher temperatures than Type I fluid inclusions for data evaluated in this study.

## TYPE V FLUID INCLUSIONS

On freezing the monophase Type V inclusions, phase separation of the vapour bubble into $CO_2$-bearing liquid

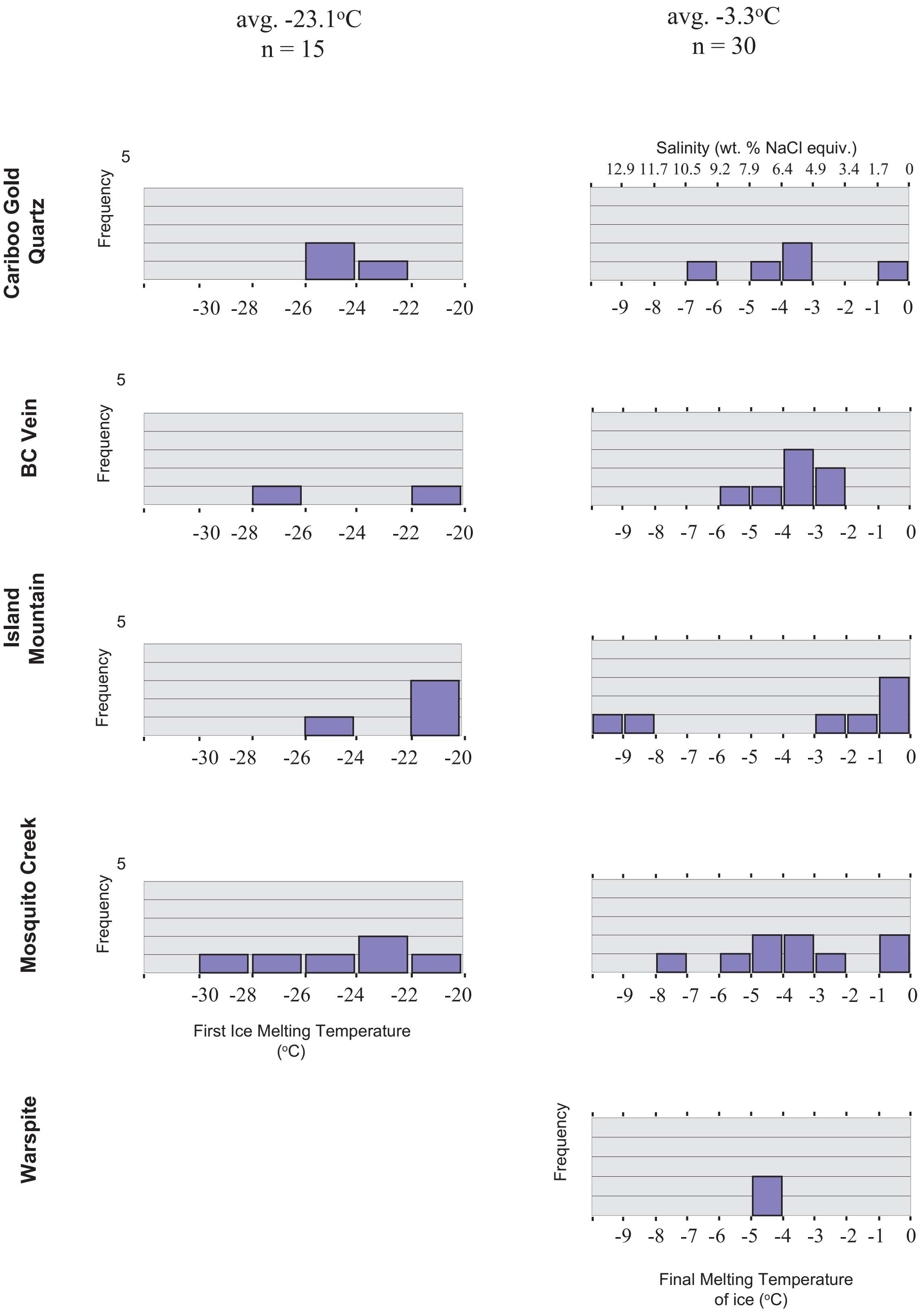

Figure 2. Temperatures of first melt and final melt of Type I (aqueous) fluid inclusions from the Cariboo Gold Quartz, Island Mountain, Mosquito Creek mines and BC and Warspite veins, respectively. The first melt approximates the eutectic temperatures of the fluid inclusions. The final melt is used to calculate the equivalent salinity. Note the diagrams share common x axes.

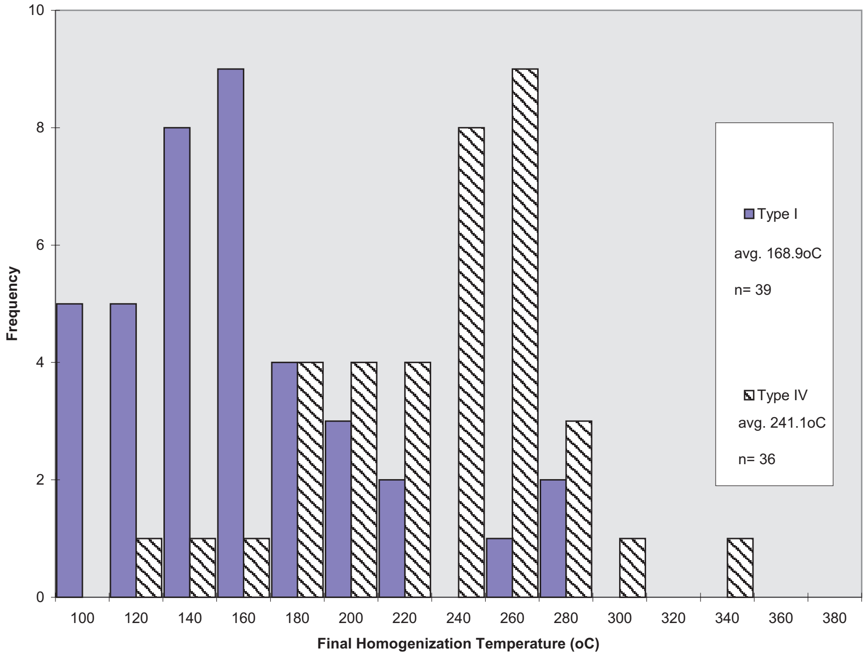

Figure 3. Type I (aqueous) versus Type IV ($CO_2$-bearing) fluid inclusion final homogenization temperatures, to the aqueous phase, in quartz from all vein and massive pyrite samples evaluated in this study.

and $CO_2$-bearing vapour phases occurred at temperatures below 20°C, often below 0°C. Further cooling resulted in freezing of the $CO_2$ phase at about -90 to -95°C. Rarely, the segregation of a second $CO_2$-rich liquid occurs at temperatures just below the freezing point. Up to 3 different stable phase transitions and rarely one metastable phase transition are observed on warming to just above room temperature ~22°C. The phase transitions observed were: initial melting (occasionally), final melting, metastable partial liquid homogenization (rarely) and final homogenization.

The first observed melting event is incipient or first melting, termed 'initial melting' by Kerkhof and Thiery (1994), which occurs as the formation of a liquid on melting solid $CO_2$ (but not complete melting of solid $CO_2$). This melt event which ranges from -94 to -69°C is observed in 6 fluid inclusions in as many samples.

The second observed melting event, observed in 25 fluid inclusions in quartz, is final melting of solid $CO_2$. Carbon-dioxide melting temperatures typically range from -84 to -56.6°C with an average of -61.1°C (Figure 5) which is significantly lower than the range and average observed for $CO_2$ melting of Type IV fluid inclusions (Figure 4). Some $CO_2$-melting temperatures in quartz from the BC Vein and Island Mountain mine are much lower than the average temperature (Figure 5).

Metastable partial liquid homogenization of fluid inclusions that have segregated a second $CO_2$-rich liquid has been observed in 2 fluid inclusions from separate samples in the BC Vein. This phase transition involves disappearance of the outer meniscus between the two $CO_2$-rich liquid phases. Fluid inclusions from the BC Vein show metastable partial liquid homogenization at -56.6 and-63.9°C respectively.

Final homogenization temperatures of $CO_2$ liquid and vapour were obtained from 22 fluid inclusions from the same samples as $CO_2$-melting temperatures. Homogenization of the inclusions (always to the liquid phase) ranges from -62.8 to 21.3°C with an average of -6.9°C (Figure 5). Final homogenization temperatures in quartz from the BC Vein and Island Mountain mine are much lower than the average temperature (Figure 5) as is the case for $CO_2$-melting temperatures (*see* above).

The measured $CO_2$ melt and homogenization temperatures are used to calculate fluid molar volumes (or the density) and composition of Type V fluid inclusions using VX diagrams of Thiery *et al.* (1994). The average $CO_2$ melt temperature of -61.1°C and average $CO_2$ homogenization temperature of -6.9°C indicates an average molar volume of 51 cubic centimetres per mol and on average < 16 mole percent $CH_4$ dissolved in the $CO_2$ (Thiery *et al.*, op. cit.). Some $CO_2$-melting and homogenization temperatures in quartz from the BC Vein and Island Mountain occurrences are much lower than the above calculated averages. These inclusions have molar volumes in the range of 51 to >100 cubic centimetres per mol and comprise from 33 to possibly > 90 mole percent $CH_4$ dissolved in the $CO_2$ (Thiery *et al.*, op cit.). The high $CH_4$ in the Type V fluid inclusions from the BC Vein and Island Mountain occurrences indicate that they are $CH_4$-dominant and represent $CH_4$-$CO_2$ fluids. When the $CH_4$-$CO_2$ fluid inclusions are removed from fluid inclusions used in the the

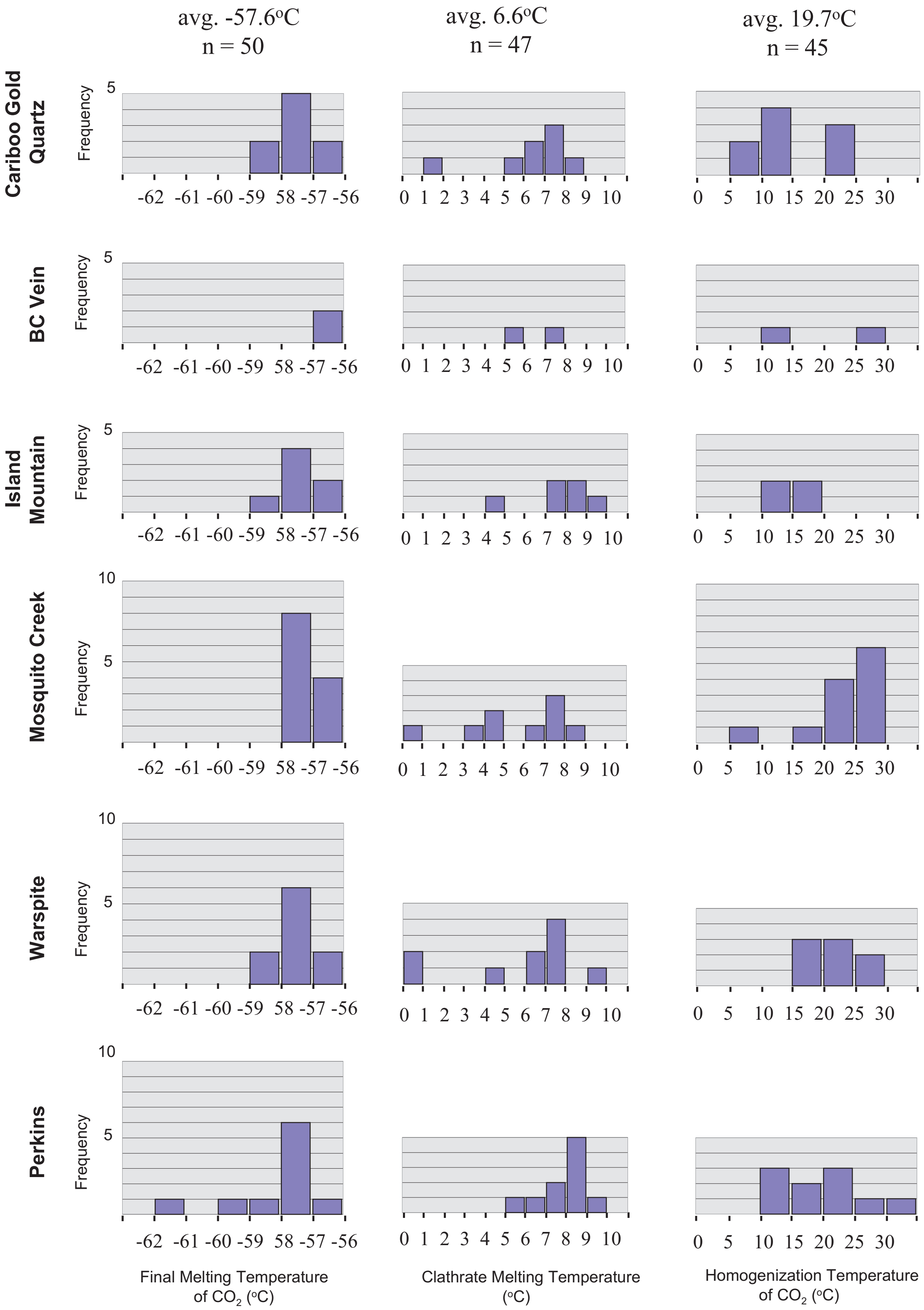

Figure 4. Temperatures of final $CO_2$ melt, clathrate melt and homogenization of $CO_2$ phases of Type IV ($CO_2$-bearing) fluid inclusions from the Cariboo Gold Quartz, Island Mountain, Mosquito Creek mines and BC, Warspite and Perkins veins, respectively. The final $CO_2$ melt temperature is used approximate the proportion of $CH_4$, $N_2$ or other volatile phases trapped in the fluid inclusions. The clathrate melt is used to calculated the equivalent salinity. The homogenization temperature of $CO_2$ is used to calculate the $CO_2$ density. Note the diagrams share common x axes.

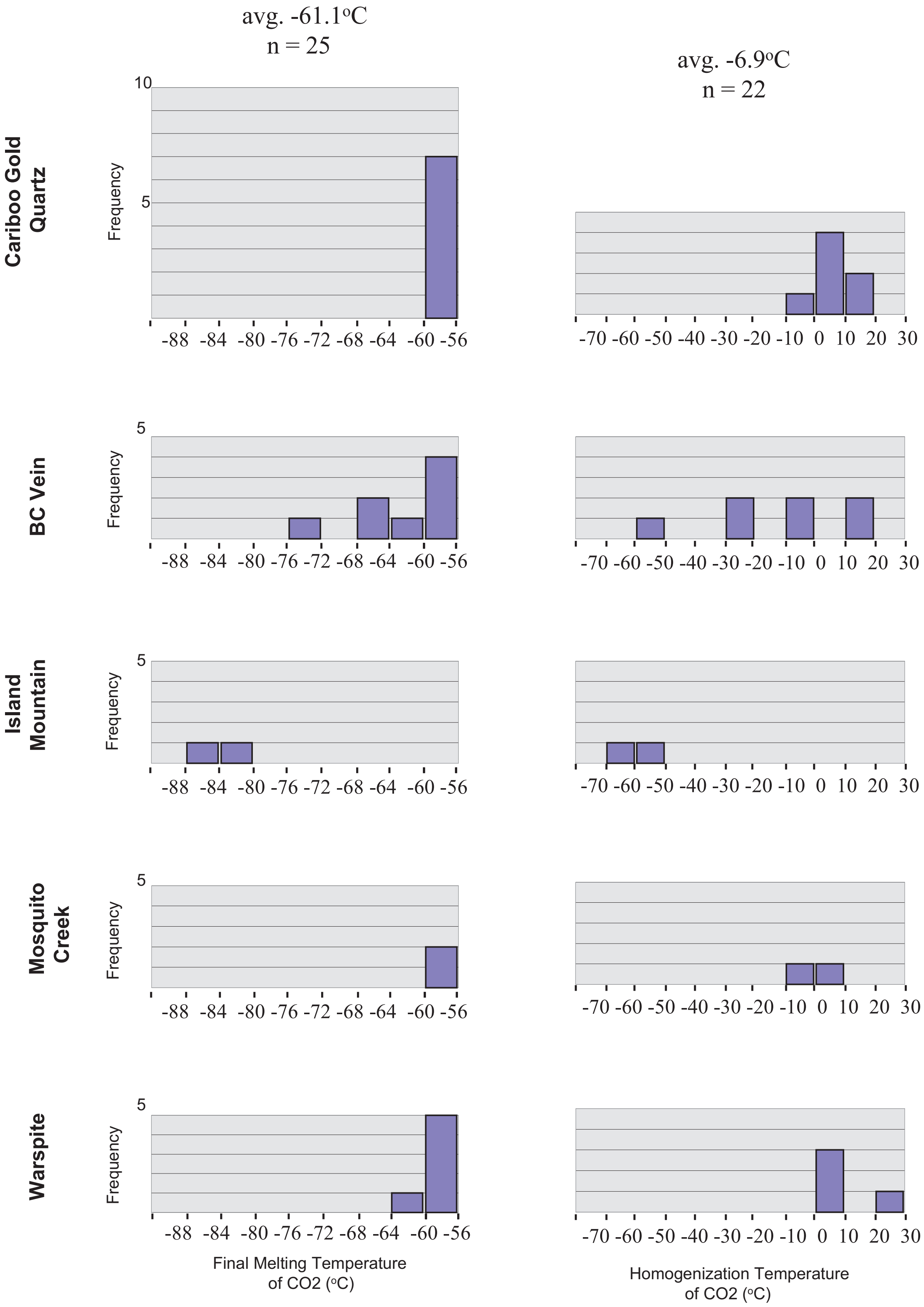

Figure 5. Temperatures of final $CO_2$ melt and $CO_2$ homogenization of Type V ($CO_2$-$CH_4$±$N_2$) fluid inclusions.

average calculation of fluid molar volume and composition for Type V fluid inclusions, the average molar volume and composition of dominantly $CO_2$-$CH_4$ fluid inclusions is 50 cubic centimetres per mol and 4 mole percent $CH_4$.

## Variation in Final Homogenization Temperature

Fluid inclusion final homogenization temperatures to the aqueous liquid phase for 75 Type I and IV fluid inclusions in quartz collected from quartz veins and massive pyrite mineralization in the 6 mineralized zones studied show virtually no difference between fluid inclusions of primary versus secondary origin (Figure 6). A wide spread in homogenization temperatures for both fluid inclusion origins range from 120 to 300°C. Fluid inclusions of indeterminate origin display a similar homogenization temperature range.

Preliminary comparison of the homogenization temperatures and composition of fluid inclusions in late (?), open-space fill quartz vugs and the earlier massive quartz were evaluated on 8 and 6 fluid inclusions from 2 quartz veins at the Mosquito Creek and Perkins deposits respectively. Types I and IV fluid inclusions in massive 'cloudy' quartz from a vein at Mosquito Creek (GR-00-67) showed salinities between 3.5 and 7.6 wt. percent equivalent NaCl and homogenization temperatures ranging from 162 to 258°C. Types I and IV fluid inclusions in 'clear' quartz from the same vein showed salinities between 2.8 and 5.1 wt. percent equivalent NaCl and homogenization temperatures ranging from 155 to 289°C. Type IV fluid inclusions in massive 'cloudy' quartz from the Perkins vein (GR-00-56) showed salinities between 2.4 and 3.9 wt. percent equivalent NaCl and homogenization temperatures ranging from 274 to 279°C. Type IV fluid inclusions in 'clear' quartz from the same vein showed salinities between 1.4 and 3.9 wt. percent equivalent NaCl and homogenization temperatures ranging from 224 to 270°C. The results of the preliminary comparison are inconclusive due to the limited data. Further detailed microthermometric work on more fluid inclusions in quartz vugs and massive quartz from a number of vein samples is needed to determine the temperature and compositional differences between these two vein textures.

Fluid inclusion final homogenization temperatures to the aqueous liquid phase for 73 Type I and IV fluid inclusions in quartz from vein and 'massive' styles of mineralization are compared in Figure 7. This figure includes homogenization temperatures from primary, secondary, pseudosecondary and intermediate fluid inclusions based on the premise that virtually no difference exists between the homogenization temperatures of fluid inclusions of primary versus secondary origin (Figure 6). The homogenization temperature range (approximately 100 to 300°C)

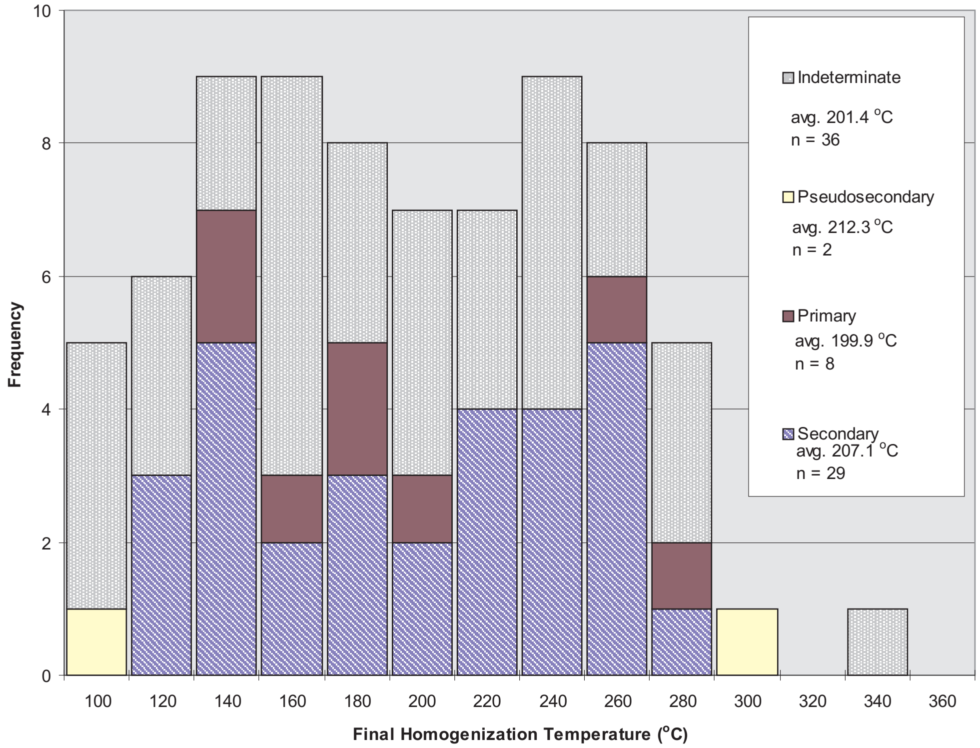

Figure 6. Distribution of primary, pseudo-secondary, secondary and indeterminate fluid inclusion origins with respect to final homogenization temperatures, to the aqueous phase, for Type I and IV fluid inclusions in quartz collected from quartz vein and massive pyrite samples from the Cariboo Gold Quartz, Island Mountain, Mosquito Creek mines and BC, Warspite and Perkins veins, respectively.

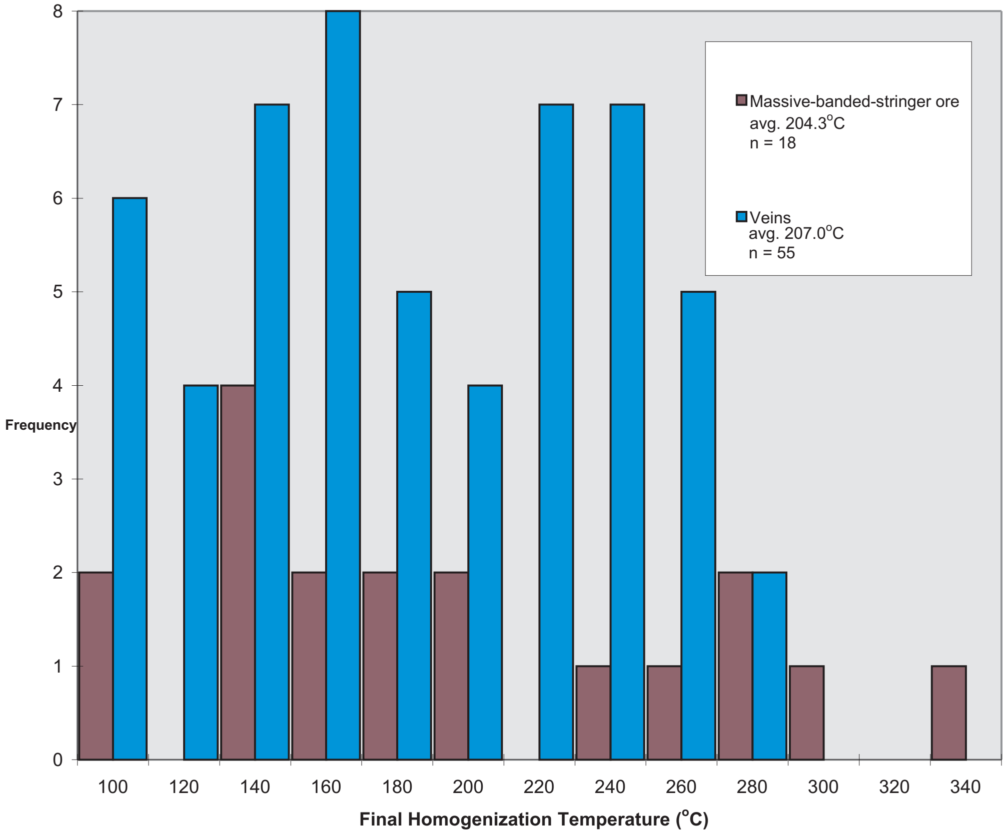

Figure 7. Distribution of final homogenization temperatures, to the aqueous phase, for Type I and IV fluid inclusions in quartz veins from the Cariboo Gold Quartz, Island Mountain, Mosquito Creek mines and BC, Warspite and Perkins veins, respectively, versus in quartz from massive-banded-stringer ore at the Island Mountain and Mosquito Creek mines.

is the same for vein and 'massive' styles of mineralization as are the homogenization temperature averages: 207 and 204°C, respectively (Figure 7). Additional analyses and comparison of homogenization temperatures for each fluid inclusion Type and direct comparison of secondary fluid inclusion origins are recommended to verify the above preliminary results.

Preliminary comparison of fluid inclusion final homogenization temperatures to the aqueous liquid phase for 75 Type I and IV fluid inclusions in quartz from samples from vein and 'massive' styles of mineralization at the Cariboo Gold Quartz, Island Mountain, and Mosquito Creek mines and the Warspite, Perkins, and BC veins are in Figure 8. Vein mineralization is indicated by fluid inclusion homogenization data represented by white and striped columns, 'massive' pyrite style mineralization by black columns. This figure includes homogenization temperatures from primary, secondary, pseudosecondary and intermediate fluid inclusions based on the premise that virtually no difference exists between the homogenization temperatures of fluid inclusions of primary versus secondary origin (Figure 6). There is virtually no difference in the homogenization temperature range of the vein and 'massive' styles of mineralization at the Island Mountain and Mosquito Creek mines (Figure 8). Both styles at Mosquito Creek show two distinct populations (100 to 180°C and 240 to 360°C). that may reflect differences due to homogenization temperatures of lower temperature Type I versus higher temperature Type IV fluid inclusions (Figure 3).

Homogenization temperatures from both the vein and 'massive' styles of mineralization are averaged in Figure 8 based on the premise that virtually no difference exists between homogenization temperatures from both styles of mineralization (Figure 7). The homogenization temperatures for the Cariboo Gold Quartz and Island Mountain mines and BC vein show remarkably consistent averages (between 180 and 192°C) although the range of homogenization temperatures are similar (approximately 120 to 300°C). Average homogenization temperatures from the Mosquito Creek mine and Warspite veins are considerably higher at 212 and 217°C respectively. Quartz in the Perkins veins have the highest average homogenization temperatures (avg. 253°C). This may reflect the absence of generally lower temperature Type I fluid inclusions (Figure 3) in quartz at the Perkins veins.

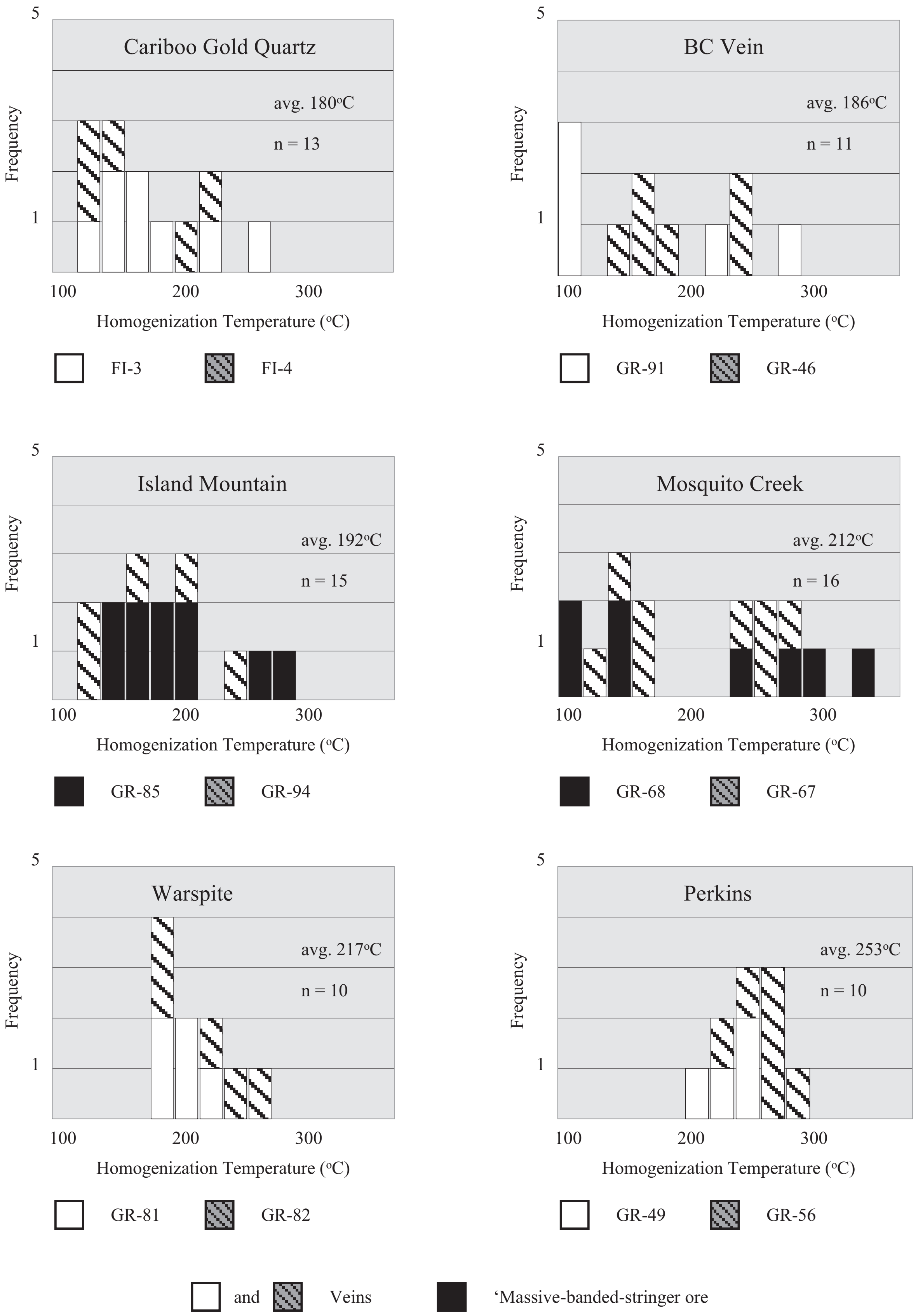

Figure 8. Final fluid inclusion homogenization temperatures (range, average and number), to the aqueous phase, for Type I and IV fluid inclusions from the Cariboo Gold Quartz, Island Mountain, Mosquito Creek mines and BC and Warspite veins, respectively. Note the diagrams share common x axes.

# DISCUSSION

This discussion focuses on the following: (1) estimated fluid properties of inclusions in quartz from both vein and 'massive' ore in the Wells-Barkerville Belt, (2) the relationship of fluid inclusions to metamorphism and the introduction of metals in these types of mineral deposits and (3) proposed analogues to the Wells-Barkerville mineralization from a fluid inclusion standpoint.

## Fluid Properties

Petrographic and microthermometric data on primary, pseudosecondary and secondary fluid inclusions in quartz from vein and 'massive' ore in the belt indicates there are four compositional types of fluid inclusions. These were identified through observation of phases present and volume percent of phases at room temperature: two-phase aqueous liquid-rich (Type I), multiphase (Type III), two and three-phase mixed aqueous and $CO_2$-rich (Type IV) and monophase $CO_{2-}$ $CH_4$ (Type V). Estimates of average composition, salinity and final homogenization temperature for each fluid inclusion type are in Table 2.

### *COMPOSITION AND SALINITY*

Type I fluid inclusions are $H_2O$-dominant with low average homogenization temperatures ($169^oC$) compared with Type IV fluid inclusions ($241^oC$). Salinities of Type I fluid inclusions are low averaging 5.4 wt. percent NaCl equiv. This type of inclusion is commonly found in submetamorphic to subgreenschist facies metamorphic rocks (Marshall *et al.*, 2000). Marshall (op. cit.) notes that $H_2O$ dominates in the uppermost continental crust but is progressively diluted by $CH_4$ and then $CO_2$ during prograde metamorphism and that $CO_2 \pm CH_4 \pm N_2$ is typical in inclusions from the lower crust and mantle. Low temperature (< $200^oC$) aqueous fluid inclusions with $H_2O$-NaCl-$CaCl_2$ composition in gold-bearing quartz vein deposits from the southeastern Abitibi Subprovince, Quebec, represent late, post-mineralizing, fresh meteoric waters that percolate downward mixing with brines (Boullier *et al.*, 1998). These deposits may be analogues to gold-bearing veins in the Wells-Barkerville Belt (*see* below).

Multiphase Type III fluid inclusions appear to be $H_2O$-dominant and some inclusions contain $CO_2$ (based on freezing behaviour). At least some of the solid phases appear to be salts which would indicated salt-saturation and minimum salinities of 26.3 wt. percent NaCl equiv. Calculations based on ice melting temperatures give approximate average salinities of 11.8 wt. percent NaCl equiv. Further work using additional analytical techniques is required to resolve the composition of this type of inclusion.

Type IV fluid inclusions fall in the category of High $XH_2O$ (Low $XCO_2$) compositional type based on compositions in Table 2 (Diamond, 1994). This type is typical of $CO_2$-$H_2O$ fluid inclusions found in low to medium grade metamorphic rocks and mesothermal to hypothermal ore deposits (Diamond, op. cit.). Marshall *et al.* (2000) suggests that $H_2O$-dominant fluid inclusions with only minor

**TABLE 2**
**SUMMARY OF FLUID INCLUSION CHARACTERISTICS FOR FLUID TYPES PRESENT IN VEINS AND MASSIVE-BANDED-STRINGER ORE IN THE WELLS-BARKERVILLE BELT**

| FI TYPE (see text) | ORIGIN[1] | BULK INCLUSION COMPOSITION (AVERAGE) | SALINITY[2] wt. percent NaCl equiv. | HOMOGENIZATION TEMPERATURE, to the aqueous phase, RANGE AND (AVERAGE)[3] in $^oC$ | ESTIMATED MINIMUM PRESSURE RANGE[4] (bars) |
|---|---|---|---|---|---|
| I | P, S | (H2O 0.98, NaCl 0.02) | 5.4<br>n=30 | 101.1 to 299 (169)<br>n = 39 | |
| III | S | (H2O 0.96, NaCl 0.04? , CO2?) | 11.8<br>n = 3<br>or > 26.3? | 224<br>n = 1 | |
| IV | S<br>(all quartz veins) | (H2O 0.85, CO2 0.13, NaCl 0.02) | 6.2<br>n = 17 | 178 to 277 (242)<br>n = 11 | 1628 to 3081<br>n = 11 |
| | P<br>(massive pyrite from IMm) | (H2O 0.93, CO2 0.05, NaCl 0.02) | 4.2<br>n = 3 | 189 to 292 (249)<br>n = 3 | 1910 to 3412<br>n = 3 |
| V | S | (CO2 0.96 , CH4 0.04) and(CH4 0.7, CO2 0.3) | | 0 | |

1. Fluid inclusion origins: P = primary, S = secondary (see text for explanation)
2. Salinity given as weight percent NaCl equivalent, n = number of analyses
3. Number of analyses for average = n
4. Number of analyses for range = n

$CO_2$ are predominant in greenschist facies metamorphic rocks.

Type V inclusions in this study are classified as homogenization or H-type inclusions (Kerkhof and Thiery, 1994) because the last phase transition observed is characterized by liquid-gas homogenization (always to the liquid phase) rather than solid-gas or solid-liquid homogenization. Type V inclusions are further subdivided into $H_3$ and $H_2$ types based on the observed differences in phase behaviour. Fluid inclusions that exhibit initial melting, final melting and final homogenization of $CO_2$-rich phases are classified as $H_3$-type (Kerkhof and Thiery, op. cit.); inclusions exhibiting final melting plus or minus metastable phase transitions followed by final homogenization of $CO_2$-rich phases are classified as $H_2$-type (Kerkhof and Thiery, op. cit.). Type $H_2$ behaviour is typical for $CO_2$-$CH_4$ mixtures and type $H_3$ behaviour is typical for $CO_2$-rich compositions (Kerkhof and Thiery, op. cit.). Fluid inclusions in this study are dominantly $H_2$-type. Based on the dominance of $H_2$-type inclusions, the $CO_2$-$CH_4$ model system, rather than the $CO_2$-$N_2$ model system, is used for Type V inclusions in this study.

The composition of type V inclusions falls in two distinct ranges: high $CO_2$ - low $CH_4$ and low $CO_2$-high $CH_4$ (Table 2). The latter high $CH_4$ composition has only been noted in secondary fluid inclusions at the BC Vein and in a vein from the Island Mountain mine.

### *MINIMUM PRESSURE ESTIMATES*

Minimum pressure estimates have been calculated for Type IV fluid inclusions using bulk density estimates for the carbonic portion of the inclusions, and projecting isochores calculated using the equation of Kerrick and Jacobs (1981) and the FLINCOR program of Brown and Hagemann (1994) to temperatures of homogenization (minimum trapping temperature estimates). Although this technique assumes binary $CO_2$-$H_2O$ mixtures, it can be applied to $CO_2$-$H_2O$ mixtures with the addition of up to 15 wt. percent NaCl equiv. (Diamond, 1994). The range in density for the $CO_2$ component of the inclusions is 0.54 to 0.84 grams per cubic centimetre (Thiery *et al.*, 1994).

The range of minimum pressures of entrapment for secondary Type IV ($H_2O$-$CO_2$-NaCl) fluid inclusions in quartz veins in the belt are 1628 to 3081 bars (Table 2). Entrapment pressures for primary Type IV fluid inclusions in quartz from massive pyritic ore at the Island Mountain mine, are 1910 to 3412 bars (Table 2). Minimum depths of formation for the secondary inclusions in quartz veins are conservatively estimated at about 6 to 12 km. Minimum depths of formation for the primary inclusions in 'massive' pyrite at the Island Mountain mine are conservatively estimated at about 7 to 13 km. Both minimum pressure estimates assume lithostatic pressure (greater depths would be inferred for hydrostatic conditions).

## Genetic Models

As intrusive rocks are extremely rare in the Wells-Barkerville Belt, a magmatic-hydrothermal source for the gold seems unlikely. However, two alternative models have been proposed for mineralization: (1) a synmetamorphic model involving the introduction of metals. In the case of the massive pyritic ore this involved replacement during or just after prograde regional metamorphism (Benedict, 1945, Skerl, 1948, Alldrick, 1983), and (2) a syn-sedimentary model involving metamorphic overprinting of sedimentary-exhalative ore (Robert and Taylor, 1989). As part of their argument, these authors suggest that Wells-Barkerville gold differs from typical mesothermal deposits because they are hosted by a dominantly sedimentary sequence and lack any spatial association with major faults or recognized shear zones.

## Relationship of Fluid Inclusions to Metamorphism

Petrographic observation indicates that primary and pseudosecondary fluid inclusions with relatively consistent liquid-to-vapour ratios but moderately variable homogenization temperatures formed in recrystallized zones around pyrite in massive-banded-stringer ore at the Mosquito Creek and Island Mountain deposits. The variability in homogenization temperature data may be due to thermal reequilibration, undetectable necking down or real variability in the FIA's. The cause of the variability is difficult to assess given the limited data available. Assuming the real variability in the FIA's and noting that the pyrite also appears to be recrystallized, it is possible that the primary and pseudosecondary inclusions may trap fluids that record metamorphic conditions during or just after peak metamorphism when the sulphides and gold were introduced as massive-banded-stringer ore.

Marshall *et al.* (2000) suggest that fluid inclusion studies of ores that are potentially metamorphosed or synmetamorphic require identification of: (1) preserved premetamorphic fluid inclusions, (2) inclusions relating to peak metamorphic conditions, and (3) inclusions relating to retrograde remobilization of ore or mineralization overprinting. Such detailed work requires evaluation of structural and metamorphic parageneses in combination with fluid inclusion paragenesis, preferably from a number of gangue and sulphide phases, to derive a fluid history. Ideally, future fluid inclusion work should examine fluid inclusions in sphalerite, scheelite and quartz in each vein set as well as the two styles of 'massive' pyritic ore in the belt.

A question to be answered is the relationship of secondary fluid inclusions in the quartz veins in the belt to the synmetamorphic introduction of metals. The similarity in composition, salinity and homogenization temperature range of primary and pseudosecondary fluid inclusions in the 'massive' style mineralization and secondary fluid inclusions in the Island Mountain and Mosquito Creek veins may be preliminary evidence that the two fluid inclusion types did trap similar metamorphic fluids. Or, perhaps the secondary inclusions record microfracture histories that postdate the main vein-filling and mineralizing fluid events. Detailed work as described above is required to resolve this question. McKeag and Craw (1989) report no significant statistical difference between the primary and secondary inclusions at the Macraes shear zone-related gold vein in the Otago Schist Belt of New Zealand. They consider the two fluid inclusion origins to have formed contemporaneously.

Criteria for local effervescence, or unmixing of a primary, homogeneous $CO_2$-$H_2O$ fluid phase, have been observed in pseudosecondary fluid inclusions in quartz from 'massive' ore at the Mosquito Creek deposit and in secondary fluid inclusions from a vein at the Cariboo Gold Quartz deposit. This mechanism coupled with evidence of gold precipitation in secondary fluid inclusion filled fractures is cited as the cause of gold mineralization in veins at the Sigma Mine in Quebec (Robert and Kelly, 1987).

## Analogues

Gold-bearing mineralization in the Wells-Barkerville Belt is not spatially associated with any plutonic rocks but is hosted by greenschist facies phyllite supracrustal rocks that have undergone early ductile and subsequent brittle deformation. Both the veins and the massive pyrite ore probably formed late in the $F_2$ ductile deformation history (Ray *et al.*, 2001, this volume).

Veins in the Mosquito Creek and Cariboo Gold Quartz deposits, specifically, have been classified as 'Au-Quartz veins' by Ash and Alldrick (1996). This broad classification includes "mesothermal" veins associated with major faults or shear zones such as the Mother Lode district in California (Weir and Kerrick, 1987), the Bralorne-Pioneer system west of Lillooet in British Columbia (Leitch *et al.*, 1988) and Archean lode gold deposits in Ontario and Quebec, for example, at the Sigma mine (Robert and Kelly, 1987).

The Otago Schist Belt of New Zealand includes two types of W-and Au-mineralized veins: (1) 'syn-metamorphic' foliation-parallel veins that formed close to the peak metamorphic temperature and post peak-pressure conditions and (2) 'post-peak metamorphic' veins which are typically hosted in extension structures (Smith and Yardley, 1999). The main difference in fluid inclusion composition between the two vein types is the presence of $CO_2$ as a major component in the post-metamorphic vein inclusions and absence of detectable $CO_2$ in the syn-metamorphic veins (Smith and Yardley, op. cit.). Post-metamorphic veins also tend to have higher salinities (up to > 9 wt. percent NaCl equiv.) rather than salinities equivalent to sea-water or less (< 3.3 wt. percent NaCl equiv.) which were recorded for syn-metamorphic veins (McKeag and Craw, 1989, Smith and Yardley, op. cit.). Fluid inclusions from all the Wells-Barkerville Belt quartz veins evaluated in this study have readily detectable $CO_2$ and salinities comparable to 'post-metamorphic lodes' (Henley *et al.*, 1976) of the Otago Schist Belt in New Zealand. Other potential analogues for Wells-Barkerville Belt veins include the 'mesothermal' veins in the Klondike District, Yukon (Rushton *et al.*, 1993), Meguma Terrane, Nova Scotia (Kontak *et al.*, 1988) and the Bendigo Gold Fields, Central Victoria, Australia (Jia *et al.*, 2000).

## SUMMARY

This preliminary study of fluid inclusions in quartz from vein and 'massive' styles of pyritic mineralization provides the following information concerning the nature of fluids that may relate to metamorphism, deformation and deposition of gold and/or late tectonic overprinting in the Wells-Barkerville Gold Belt:

- Some veins in the belt exhibit wispy quartz textures indicating deep (> 4 km) environments and other veins exhibit breccia and open-space filling textures indicating (later?) deposition at more shallow levels (< 1-3 km?) environments. In some veins, both deep and shallow textures are observed.
- Quartz in the quartz-pyrite veins contain fluid inclusions of mostly secondary origin. It is not clear whether some secondary inclusions have trapped metamorphic fluids or whether they record microfracture histories that postdate the main vein-filling and mineralizing fluid events.
- Quartz in the massive-banded-stringer pyrite ore includes variable proportions of very fine-grained, possibly recrystallized or highly strained quartz that contains primary and pseudosecondary fluid inclusions. These fluid inclusions may trap fluids that record synmetamorphic conditions at the time of sulphide and gold deposition.
- The following four compositional types of fluid inclusions are identified in the vein and 'massive' styles of mineralization based on phases present at room temperature and microthermometric data: Type I: 'Aqueous' $H_2O$-NaCl, Type III: 'Multiphase' $H_2O$-NaCl ($\pm CO_2$), Type IV: '$CO_2$-bearing' $H_2O$-$CO_2$-NaCl and Type V: '$CO_2$-$CH_4$' $CO_2$-$CH_4$ ($\pm N_2$) or '$CH_4$>$CO_2$'.
- The dominant fluid inclusion types in both the vein and 'massive' mineralization are Type I and Type IV.
- Type I inclusions have average bulk composition (mole percent) of approximately 98% $H_2O$ and 2% NaCl.
- Type IV secondary inclusions from veins have an average bulk composition (mole percent) of about 85% $H_2O$, 13% $CO_2$ and 2% NaCl.
- Type IV primary inclusions from 'massive' mineralization at the Island Mountain mine have average bulk composition (mole percent) of approximately 93% $H_2O$, 5% $CO_2$ and 2% NaCl. This composition is significantly different from the composition of Type IV secondary fluid inclusions in veins.
- Overall, Type IV fluid inclusions homogenize at significantly higher final temperatures (avg. 241$^{o}$C) than Type I fluid inclusions (avg. 169$^{o}$C).

- No significant differences are seen between primary and secondary fluid inclusion final homogenization temperatures for Type I and Type IV fluid inclusions.
- No significant differences are seen in final homogenization temperature in the vein and ‘massive’ styles of mineralization, either in the same deposits or between deposits.
- Quartz in the Perkins veins has different fluid inclusion characteristics from other veins in the belt. It is characterized by Type III and IV fluid inclusions that homogenize at significantly higher temperatures (avg. $253^{o}$C) than the other vein deposits studied which average < $220^{o}$C. Type I and V fluid inclusions are notably absent in the Perkins veins.
- The range of minimum pressures of entrapment for secondary Type IV ($H_2O$-$CO_2$-NaCl) fluid inclusions in veins from the Cariboo Gold Quartz mine and BC, Warspite and Perkins veins are 1628 to 3081 bars. Minimum depths of formation are conservatively estimated at about 6 to 13 km, assuming lithostatic pressure
- The range of minimum pressures of entrapment for primary Type IV ($H_2O$-$CO_2$-NaCl) fluid inclusions in massive ore from the Island Mountain mine are 1910 to 3412 bars. Minimum depths of formation are conservatively estimated at about 7 to 12 km, assuming lithostatic pressure
- This fluid inclusion study suggests that the Wells-Barkerville gold-bearing veins are analogues to the ‘post-metamorphic’ gold-bearing veins in the Otago Schist Belt of New Zealand.

## ACKNOWLEDGMENTS

International Wayside Gold Mines Ltd. are thanked for permission to collect samples at the BC Vein, Cariboo Gold Quartz, Island Mountain and Mosquito Creek deposits. In particular, Richard Hall is thanked for field discussions concerning the Mosquito Creek deposit and providing access to underground workings at the Island Mountain Mine. We appreciate the help of Claude Blagdon who led us underground at the Island Mountain Mine to collect samples. Kika Ross of Panterra Geoservices Inc. is thanked for providing the sphalerite-bearing drill-core sample GR-00-91 from the BC Vein. We appreciate the editorial reviews by Nick Massey and Ian Webster; the latter is also thanked for geological discussions and help with the drafting .

## REFERENCES

Alldrick, D.J. (1983): The Mosquito Creek Mine, Cariboo Gold Belt, B.C.; in Geological Fieldwork 1982, *British Columbia Ministry of Energy, Mines and Petroleum Resources*, Paper 83-1, pages 98-112.

Ash, C. and Alldrick, D. (1996): Au-quartz Veins; in Selected British Columbia Mineral Deposit Profiles, Volume 2 - Metallic Deposits, Lefebure, D.V. and Höy, T., Editors, *British Columbia Ministry of Employment and Investment*, Open File 1996-13, pages 53-56.

Benedict, P.C. (1945): Structure at Island Mountain Mine, Wells, B.C.; *Canadian Institute of Mining and Metallurgy*, Transactions, Volume 48, pages 755-770.

Bodnar, R.J. (1993): Revised equation and table for determining the freezing point depression of H2O-NaCl solutions; *Geochimica et Cosmochimica Acta*, Volume 57, pages 683-684.

Bodnar, R.J., Reynolds, T.J. and Kuehn, C.A. (1985): Fluid-Inclusion Systematics in Epithermal Systems; in Geology and Geochemistry of Epithermal Systems, Berger, B.R. and Bethke, P.M., Editors, *Mineralogical Society of America*, Reviews in Economic Geology, Volume 2, pages 73-97.

Boullier, A-M., Firdaous, K. and Robert, F. (1998): On the Significance of Aqueous Fluid Inclusions in Gold-Bearing Quartz Vein Deposits from the Southeastern Abitibi Subprovince (Quebec, Canada); *Economic Geology*, Volume 93, pages 216-223.

Brown, P.E. and Hagemann, S.G. (1994): MacFlincor: a computer program for fluid inclusion data reduction and manipulation; in Fluid Inclusions in Minerals: Methods and Applications, Short Course of the Working Group (IMA) “Inclusions in Minerals”, De Vivo, B. and Frezzotti, M.L., Editors, *Virginia Polytechnic Institute and State University*, pages 231-250.

Brown P.E. and Lamb W.M. (1989): P-V-T properties of fluids in the system $H_2O$-$CO_2$-NaCl: New graphical presentations and implications for fluid inclusion studies; *Geochimica et Cosmochimica Acta*, Volume 53, 1209-1221.

Burruss, R.C. (1981): Analysis of Phase Equilibrium in C-O-H-S fluid inclusions; in Short Course in Fluid Inclusions: Applications to Petrology, Hollister, L.S. and Crawford, M.L., Editors, *Mineralogical Association of Canada*, Volume 16, pages 39-74.

Diamond, L.W. (1994): Introduction to phase relations of CO2-H2O fluid inclusions; in Fluid Inclusions in Minerals: Methods and Applications, Short Course of the Working Group (IMA) “Inclusions in Minerals”, De Vivo, B. and Frezzotti, M.L., Editors, *Virginia Polytechnic Institute and State University*, pages 131-158.

Gabrielse, H. (Comp.) (1991): Structural styles, Chapter 17; in Geology of the Cordilleran Orogen in Canada; Gabrielse, H. and Yorath, C.J., Editors, *Geological Survey of Canada*, Geology of Canada, Number 4, pages 571-675.

Garba, I. and Akande, S.O. (1992): The Origin and Significance of Non-Aqueous CO2 Fluid Inclusions in the Auriferous Veins of Bin Yauri, northwestern Nigeria; *Mineralium Deposita*, Volume 27, pages 249-255.

Giles, A.D. and Marshall, B. (1994): Fluid-inclusion studies on a multiply deformed, metamorphosed volcanic-associated sulfide deposit, Joma mine, Norway; *Economic Geology*, Volume 89, p. 803-819.

Goldstein, R.H. and Reynolds, T.J. (1994): Systematics of Fluid Inclusions in Diagenetic Minerals; *Society for Sedimentary Geology*, Short Course 31, 199 pages.

Guha, J., Lu, H-Z., Dube, B., Robert, F. and Gagnon, M. (1991): Fluid Characteristics of Vein and Altered Wall Rock in Archean Mesothermal Gold Deposits; *Economic Geology*, Volume 86, pages 667-684.

Hanson, G. (1935): Barkerville Gold Belt, Cariboo District, British Columbia; *Geological Survey of Canada*, Memoir 181, 42 pages.

Henley, R.W., Norris, R.J. and Paterson, C.J. (1976): Multistage Ore Genesis in the New Zealand Geosyncline A History of Post-Metamorphic Lode Emplacement; *Mineralium Deposita*, Volume 11, pages 180-196.

Holland, S.S. (1948): Report on the Stanley Area Cariboo Mining Division; *British Columbia Department of Mines*, Bulletin 26, 66 pages.

International Wayside Gold Mines Ltd. (2000): Cariboo Gold Project Application to British Columbia Ministry of Energy and Mines under Environmental Assessment Act.

Jia, Y., Li, X. and Kerrich, R. (2000): A Fluid Inclusion Study of Au-Bearing Quartz Vein Systems in the Central and North Deborah Deposits of the Bendigo Gold Field, Central Victoria, Australia; *Economic Geology*, Volume 95, pages 467-494.

Johnson, W.A. and Uglow, W.L. (1926): Placer and Vein Gold Deposits of Barkerville, Cariboo District, British Columbia; *Geological Survey of Canada*, Memoir 149, 246 pages.

Kerkhof, F. van den and Thiery, R. (1994): Phase Transitions and Density Calculation in the CO2-$CH_4$-$N_2$ System; in Fluid Inclusions in Minerals: Methods and Applications, Short Course of the Working Group (IMA) "Inclusions in Minerals", De Vivo, B. and Frezzotti, M.L., Editors, *Virginia Polytechnic Institute and State University,* pages 171-190.

Kerrick D.M. and Jacobs G.K. (1981): A modified Redlich-Kwong equation for $H_2O$, $CO_2$ and $H_2O$-$CO_2$ mixtures at elevated pressures and temperatures; *American Journal of Science*, Volume 281, pages 735-767.

Kontak, D.J., MacDonald, D. and Smith, P.K. (1988): Fluid Inclusion Study of the Beaver Dam Gold Deposit, Meguma Terrane, Nova Scotia; in Report of Activities 1988, Part A, *Nova Scotia Mines and Minerals Branch*, Report 88-3, pages 63-69.

Leitch, C.H.B., Godwin, C.I. and Brown, T.H. (1989): Characteristics of Mineralizing Fluids in the Bralorne-Pioneer Mesothermal Gold Vein Deposit: Results of a Fluid Inclusion, Stable Isotope, and Thermodynamic Study; in Geological Fieldwork 1988, *British Columbia Ministry of Energy, Mines and Petroleum Resources*, Paper 1989-1, pages 365-375.

Marshall, B., Giles, A.D. and Hagemann, S.G. (2000): Fluid Inclusions in Metamorphosed and Synmetamorphic (Including Metamorphogenic) Base and Precious Metal Deposits: Indicators of Ore-Forming Conditions and/or Ore-Modifying Histories?; in Metamorphosed and Metamorphogenic Ore Deposits, Spry, P.G., Marshall, B. and Vokes, F.M., Editors, *Mineralogical Society of America*, Reviews in Economic Geology, Volume 11, pages 119-148.

McKeag, S.A. and Craw, D. (1989): Contrasting Fluids in Gold-Bearing Quartz Vein Systems Formed Progressively in a Rising Metamorphic Belt: Otago Schist, New Zealand; *Economic Geology*, Volume 84, pages 22-33.

McTaggart, K.C. and Knight, J. (1993): Geochemistry of Lode and Placer Gold of the Cariboo District, B.C.; *British Columbia Ministry of Energy, Mines and Petroleum Resources*, Open File 1993-30, 26 pages.

Ray, G.E., Webster, I.C.L., Lane, R., Ross, K. and Hall, R. (2000): Geochemistry of auriferous pyrite mineralization at the Bonanza Ledge, Mosquito Creek Mine and other properties in the Wells-Barkerville area, British Columbia; *British Columbia Ministry of Energy and Mines*, Geological Fieldwork 2000, Paper 2001-1, this volume.

Reynolds, T.J., (1991): Short Course on Fluid Inclusions; *Mineral Deposit Research Unit*, Short Course 6.

Richards, F. (1948): Cariboo Gold Quartz Mine; in Structural Geology of Canadian Ore Deposits, *Canadian Institute of Mining and Metallurgy*, pages 162-168.

Robert, F. and Kelly, W.C. (1987): Ore-forming fluids in Archean gold-bearing quartz veins at the Sigma mine, Abitibi Greenstone Belt, Quebec, Canada; *Economic Geology*, Volume 82, pages 1464-1482.

Robert, F. and Taylor, B.E. (1989): Structure and Mineralization at the Mosquito Creek Gold Mine, Cariboo District, B.C.; in Structural Environment and Gold in the Canadian Cordillera, *Geological Association of Canada*, Cordilleran Section, Short Course 14, 174 pages.

Roedder E. (1984): Fluid Inclusions; *Mineralogical Society of America*, Reviews in Mineralogy, Vol. 12, Bookcrafters Inc., Chelsea, Michigan, 644 pages.

Rushton, R.W., Nesbitt, B.E., Muehlenbachs, K. and Mortensen, J.K. (1993): A Fluid Inclusion and Stable Isotope Study of Au Quartz Veins in the Klondike District, Yukon Territory, Canada: A Section through a Mesothermal Vein System; *Economic Geology*, Volume 88, pages 647-678.

Rhys, D. (2000): The Cariboo Gold Project of International Wayside Gold Mines; *Vancouver Mineral Exploration Group*, Abstract, November 29, 2000, 2 pages.

Rhys, D.A.E. and Ross, K.V. (2000): Report on Petrography, Check Sampling and Geological Interpretation of Drill Core at the Bonanza Ledge Zone, Cariboo Gold Quartz Property, British Columbia; Prepared for International Wayside Gold Mines Ltd. by *Panterra Geoservices Inc*. at *http://www.wayside-gold.com/i/pdf/PanterraGeoReport_new.pdf,* 77 pages.

Skerl, A.C. (1948): Geology of the Cariboo Gold Quartz Mine, Wells, B.C.; *Economic Geology*, Volume 43, pages 571-597.

Smith, M.P. and Yardley, B.W.D. (1999): Fluid Evolution during Metamorphism of the Otago Schist, New Zealand: (I) Evidence from fluid inclusions; *Journal of Metamorphic Geology*, Volume 17, pages 173-186.

Struik, L.C. (1988): Structural Geology of the Cariboo Gold Mining District, East-Central British Columbia; *Geological Survey of Canada*, Memoir 421, 100 pages.

Sutherland-Brown, A. (1957): Geology of the Antler Creek Area, Cariboo District, British Columbia; *British Columbia Department of Mines*, Bulletin 38, 105 pages.

Thiery, R., van den Kerkhof, A.M. and Debussy, J. (1994): VX Properties of $CH_4$-$CO_2$ and $CO_2$-$N_2$ fluid inclusions; Modelling for T<31 degrees C and P< 400 bars; European Journal of Mineralogy, Volume 6, Number 6, pages 753-771.

Weir, R.H. Jr. and Kerrick, D.M. (1987): Mineralogic, Fluid Inclusion, and Stable Isotope Studies of Several Gold Mines in the Mother Lode, Tuolumne and Mariposa Counties, California; *Economic Geology*, Volume 82, p. 328-344.

Yardley, B. (1999): Discussion of inclusion survival in sheared quartz; FI Discussion Archives at http://www.geology.wisc.edu/%7Epbrown/fi.html